A Comparative Study of Ground and Satellite Evapotranspiration Models for Southern California

by

Jeffrey K. Snoddy

A Thesis Presented to the
Faculty of the USC Graduate School
University of Southern California
In Partial Fulfillment of the
Requirements for the Degree
Master of Science
(Geographic Information Science and Technology)

December 2018

Dedicated to the members of my biggest fan club, consisting of “Little One”, Bailey, Noriko, and Marshmallow. They have supported me the entire way, despite the time I have spent away from home. Though I stumbled and felt frustrated at times, not once did they think I could fail.

Table of Contents

List of Figures

List of Tables

Acknowledgements

I would like to thank my primary advisers consisting of Drs. Darren Ruddell, John Wilson, Andrew Marx, Elisabeth Sedano, and Vanessa Osborne and the many instructors throughout my time in this program. They provided proper feedback, established parameters for my study, and tightened my focus. Special thanks go out to Ken Watson who guided me through the start of my application process.

List of Abbreviations

ASCE	American Society of Civil Engineering
AWS	Amazon Web Services
℃	Celsius
d	Solar Declination
dr	Relative Distance Earth-Sun
DT	Delta Term (auxiliary calculation for Radiation Term)
ea	Actual Vapor Pressure
ENVI	Environment for Visualizing Images
ESRI	Environmental Systems Research Institute
ET_o	Reference Evapotranspiration Value
ETrad	Radiation Term
ETwind	Wind Term
EWRI	Environmental and Water Resource Institute
F	Fahrenheit
FAO – 56	Food and Agriculture Organization Irrigation and Drainage Paper 56
GIS	Geographic Information Systems
K	Kelvin
LAEMD	Los Angeles Emergency Management Department
LAI	Leaf Area Index
LCDM	Landsat Data Continuity Mission
MNWD	Moulton Niguel Water District
MODIS	Moderate Resolution Imaging Spectroradiometer

NDVI	Normalized Difference Vegetation Index
P	Atmospheric Pressure
PT	Psi Term (auxiliary calculation for wind Term)
Ra	Extraterrestrial Radiation
Rc	Canopy resistance to vapor transit (sm-1)
Rn	Net Radiation
Rnl	Net Outgoing Long Wave Solar Radiation
Rns	Net Shortwave Radiation
Rs	Mean Daily Solar Radiation
Rso	Clear Sky Radiation
SAVI	Soil-adjusted Vegetation Index
TT	Temperature Term (auxiliary calculation for Wind Term)
u2	Wind Speed
WDVI	Weighted Difference Vegetation Index
Δ	Slope of Saturation Vapor Pressure Curve
γ	Psychrometric Constant
φ	Latitude
ω	Sunset Hour Angle

Abstract

This project offers a comparative study between a ground-based weather station and satellite-based method of calculating evapotranspiration (ET). Using four selected cloudless days measured between 10:28 am and 11:30 am DST local in Los Angeles in 2016 (08 February, 19 April, 22 June, and 08 July), the aim of this project is to determine if the Normalized Difference Vegetation Index (NDVI) Triangle method, a satellite-based methodology, could be used as an acceptable alternative to measure ET for locations without a ground-based weather station.

The Moulton Niguel Water District (MNWD), located in Orange County, California was selected as the study area for this project. Weather station #245, located on the Coto De Caza golf course, generated the ground-based weather data for the Penman-Monteith calculation of evapotranspiration for the MNWD. In contrast, the satellite method used the Landsat Data Continuity Mission's (LDCM) multispectral and thermal bands to calculate ET by Land Surface Temperature (LST) and NDVI values. These two data inputs, by the application of band math, were combined to create a two-dimensional NDVI Triangle pixel plot evapotranspiration estimate for each day calculated. The data from the two methodologies were then compared, with the assumption the Penman-Monteith method was the most accurate measure of ET.
The results were statistically compared and analyzed for accuracy through Root Mean Square Error (RMSE), Mean Absolute Deviation (MAD), Mean Absolute Percentage Error (MAPE) and the coefficient of determination calculations. The results, although limited by sample size, indicate the NDVI Triangle method can be used to estimate ET. The process of creating the NDVI Triangle 2-D plot from multispectral and thermal bands from the LDCM is presented in detail, in addition to the process of defining the dry and wet edges of the plotted NDVI Triangle.

Chapter 1 Introduction

Governor Jerry Brown's Executive Order B-37-16 stipulated that California's water retailers must reduce urban water use by 20% by the year 2020. This project researches how to meet that 20% reduction of urban water use through a comparison calculation of evapotranspiration models. This project compares local ET measurement with ground-based weather stations to large-scale ET measurement through orbiting satellites.

1.1 Motivation

On 17 January 2014, Governor Jerry Brown declared a drought state of emergency to reflect the status of the reservoirs and lakes, which were below their record low with the snowpack 20 percent below average. In addition, Executive Order B-29-15 imposed restrictions to achieve a 25% reduction in urban water use and replace 50 million square feet of lawns with drought-resistant landscapes (Marcus et al. 2018). This executive order was executed successfully with an achievement of near the 25% reduction target for urban water use. Governor Brown then issued Executive Order B-37-16 to continue to build upon that success. Executive Order B-37-16 created long-term water conservation measures and set a new urban water use target of 20 percent reduction by the year 2020 (Marcus et al. 2018). On 07 April 2017, due to heavy precipitation conditions, lowered temperatures, and heavy snow fall, Governor Brown issued Executive Order B-40-17, declaring the drought over in but four California Counties: Fresno, Tulare, Kings, and Tuolumne (Marcus et al. 2018).

Figure 1 Ten hydrologic regions for the State of California
(Source https://water.usgs.gov/edu/watercycleevapotranspiration.html)

This thesis focuses on hydrological region four, which is where the MNWD is located as seen in Figure 1. The State of California has continually adjusted to the depreciation of urban water supplies in the event of a drought. Executive B-37-16 was created to mitigate an overuse of water by setting new urban water conservation targets for California's urban water retailers.

Instead of using a percentage from a baseline to measure water savings, the unique climate demographic and land-use characteristic of each urban service area will be the new standard of the measure of successful adherence to Executive Order B-37-16 (Marcus et al. 2018). This order states:

> The water use targets shall be customized to the unique conditions of each water agency, shall generate more statewide water conservation than existing requirements, and shall be based on strengthened standards for:
>
> A. Indoor residential per capita water use;
> B. Outdoor irrigation, in a manner that incorporates landscape area, local climate, and new satellite imagery data;
> C. Commercial, industrial, and institutional water use; and
> D. Water lost through leaks (Marcus et al. 2018).

The new urban water reduction methods are individually based on how the different water districts intend to apply water reduction initiatives. California population trends are creating areas of heavy irrigation, high population and increasing population density. Gleick (1998) observes large urban growth has been supported by sourcing water from out-of-state urban water regions, like the Colorado River via the Colorado River Aqueduct, and snowpack levels for in-state demands requirements. Approximately 50 percent of the water used throughout Orange County

comes from imported supplies (MWDOC 2017). California conservation efforts are critical if we are to lessen reliance on external water supplies. Evapotranspiration, which dictates how much water is needed for an irrigable field to remain fertile, is a critical key point for reducing urban water use per the Executive Directive B-37-16.

Urban water conservation efforts have been very active for the State of California. The primary user of urban water is outdoor irrigation and irrigated agriculture. The motivation to conserve water, especially saving from outdoor use, is to create more water available for residential areas and the environment. Gleick et al. (2003) estimated, in 2003, that a 25-40 percent reduction in outdoor residential water use, (360,000 – 580,000 acre/feet per year) could be conserved if the proper conservation efforts were put in place.

Entities with a large space to irrigate, the primary way to determine the amount of water to ensure their crops stay fertile or golf greens stay playable without the waste of water resources, is by using and acting upon the value of calculated evapotranspiration. That is obtained through a variety of methodologies with acquired data specifically for that microclimate.

This project seeks to discover if the NDVI Triangle, a versatile method with the ability to cover large geographical areas from space, can be utilized as an acceptable method for accurately calculating ET. This will be determined by comparing ET values obtained from the LDCM to the California Irrigation Management Information System (CIMIS) weather station #245 (Coto de Caza) which uses the Penman-Monteith Method for ET calculation. The accuracy and feasibility of this new method will be decided by statistical analysis. All CIMIS weather stations in California and, for the most part, the remainder of the world, uses the Penman-Monteith model to measure and calculate Evapotranspiration (Temesgen et al. 2018).

Evapotranspiration is the measure of how quickly, over time, water is evaporated from a defined vegetated surface (Zotarelli et al. 2009). Evapotranspiration (ET) is therefore a term that explains surface water loss by two processes: evaporation and transpiration. Evaporation is the process by which liquid waters is converted to water vapor from land surfaces and lakes, while transpiration is the process of the vaporization of water within a plant and plant stomata (Zotarelli et al. 2009). Transpiration and evaporation happen simultaneously and cannot be separated as two individual actions for evapotranspiration as seen in Figure 2. An accurate reference evapotranspiration, or better recognized as ET, is vital to reduce over and under use of water for irrigated surfaces. This may serve as an urban water use indicator to ensure as much water as possible is being conserved when irrigating.

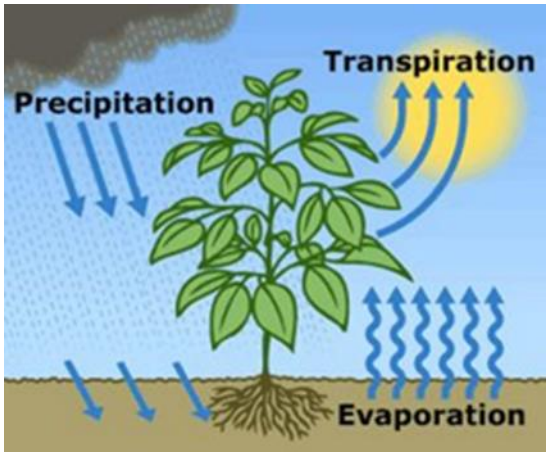

Figure 2 The process of evapotranspiration via water loss by evaporation and transpiration (Source https://water.usgs.gov/edu/watercycleevapotranspiration.html)

In line with supply chain resiliency research performed for sectors critical to the City of Los Angeles by the Los Angeles Emergency Management Department (LA EMD) in collaboration with a Federal Emergency Management Agency Technical Assistance Team (FEMA-TA), this project looks for ways to decrease the waste of urban water resources. This is to be done by establishing and proving the most versatile and acceptably accurate way to measure ET in areas, without a local

means to measure, by comparative studies. As water resources are at a premium, we need to conserve water, fill our reservoirs, and establish a set of guidelines for urban water use in preparation for our next drought.

California has suffered greatly from extreme drought conditions from 2007-2009 and 2011-2017, with conditions that have not been seen for over 1,200 years. (Griffin and Anchukaitis 2014). California's drought conditions were further exacerbated by the increased temperature and the lack of precipitation in California as seen in Figure 3 and 4. When there is a lack of rain accompanied by high temperatures as seen in Figure 5, the combination of low precipitation and increased heat leads to a greater probability of a higher occurrence of drought conditions (Diffenbaugh, Swain and Touma 2015). In addition, ET will increase, assuming water is available for transmission into the atmosphere.

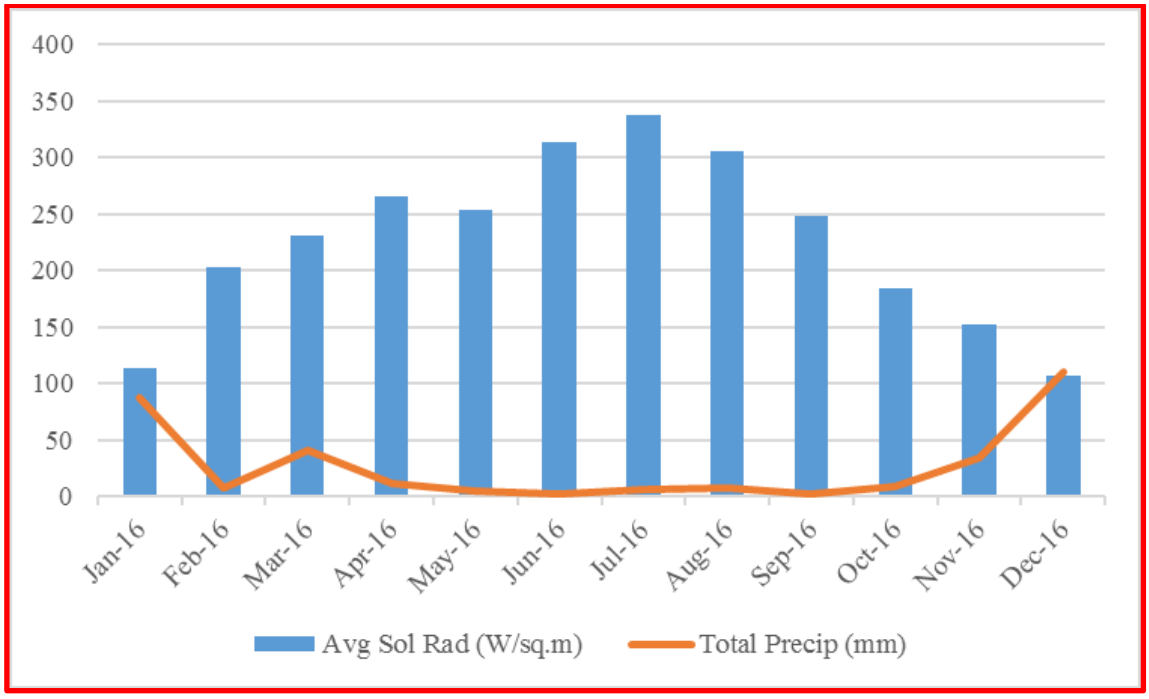

Figure 3 Plot showing MNWD's average solar radiation and precipitation for 2016 (Source: Temesgen et al. 2018)

This study aims to advance Governor Jerry Brown's Executive Directive B-37-16 which sets new water efficiency targets for California's urban water retailers. By calculating the best reference ET for irrigable areas, which is a large percentage of water usage in California and is a main target in the urban water reduction plan, irrigation can be turned off when unneeded. The calculation of ET reduces overwatering and decreases the waste of our water resources by the largest water users. This study explores the possibility of a reflective reference and a geographically expansive ET value, for areas without a ground-based weather station, using satellite imagery. Executive Directive B-37-16 intends to preserve more water resources for urban users in the event of another drought. In addition, this directive anticipates continued population growth for the State of California.

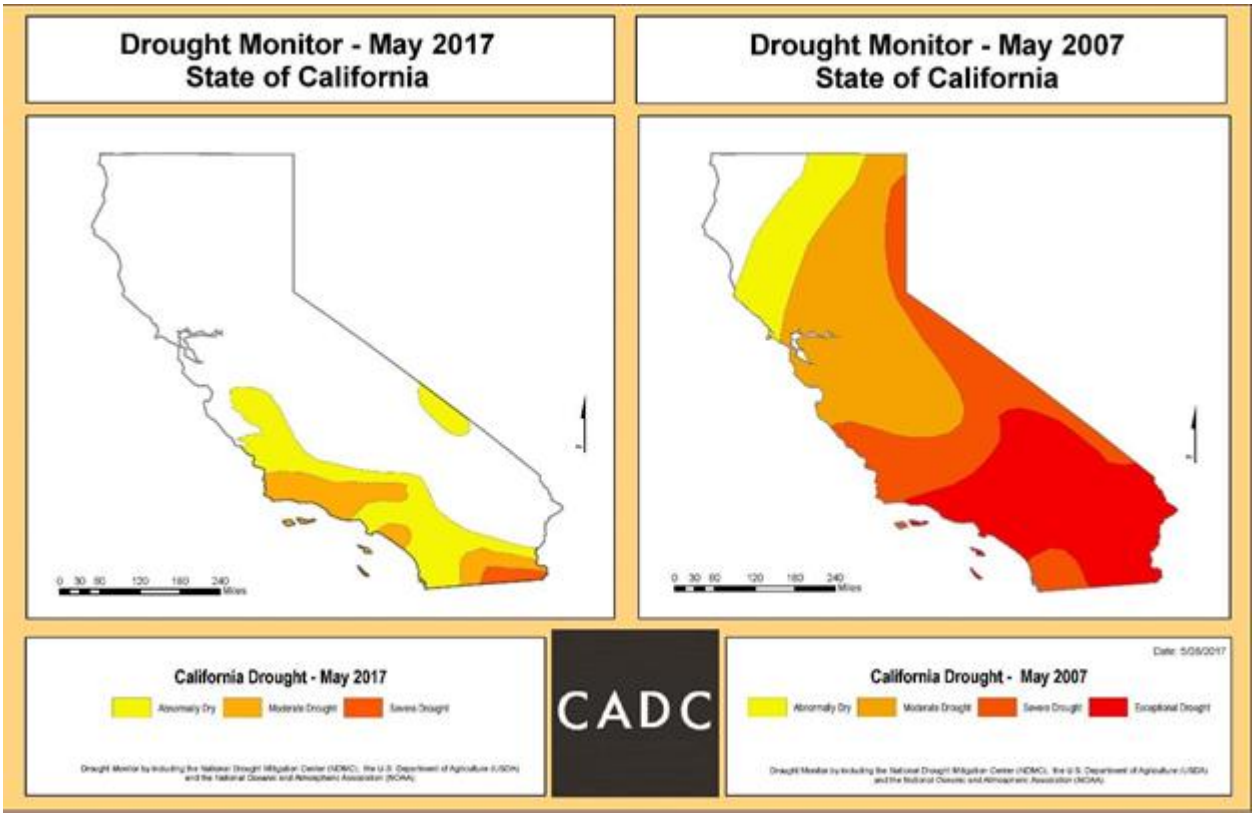

Figure 4 California drought conditions year comparison (May 2007 vs May 2017) (Source: Blunden 2018)

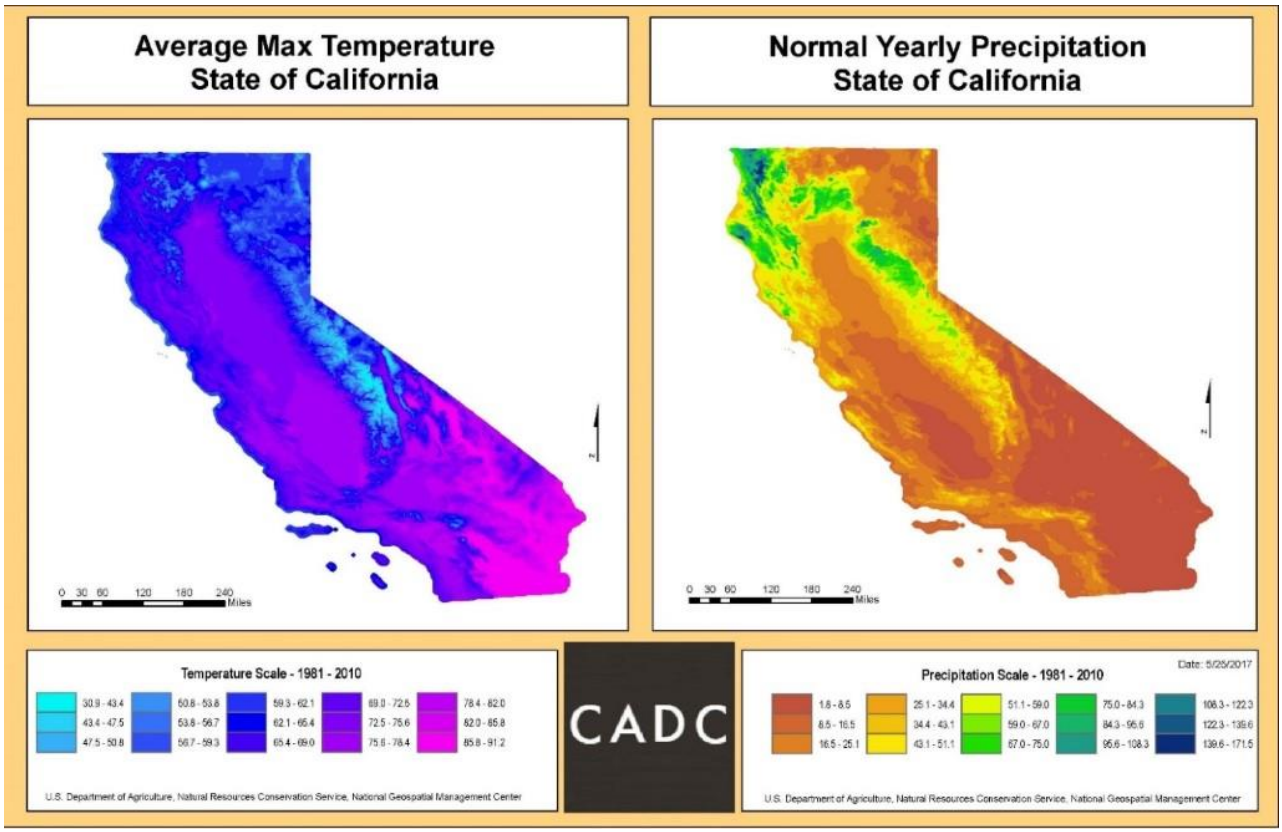

Figure 5 Processed annual maximum temperature & normal yearly precipitation from 1981 to 2010
(Source: McCarthy 2017)

California is the most populous State in the United States, with a population of nearly 40 million and grew at 0.7% in 2017 (Crane et al. 2018). Though not directly part of this project, California's progressive population growth continues to place a strain upon the State's water resources. The increase in residents has also increased the density of population centers within the city. This, in turn, has created even a greater demand for water. The population of California went from 10 million residents in 1950 to more than 39 million residents in 2016 and the state's population is predicted to reach 50 million residents by the year 2050 (Johnson 2017). There are extremely heavily populated centers within the state that creates a need for resources sustainment, preservation, and conservation. This large California population base creates an extreme need for

urban water resources in an area that naturally, not sustainable as an independent water supply node.

Precisely calculating urban water use in California is very challenging. It is an extremely complex system with diverse supply and demands nodes with multiple owners and complicated interoperability systems and processes. This adds a great deal of difficulty in achieving California's urban water use targets as set by the Governor. For example, potable and non-potable sources for California is a combination of imported water, local groundwater, reclaimed water, and recycled water. Water supply flows from water desalination plants, precipitation, ground water, purchased water, surface water, and water storage supplies as seen in Figure 6 (Allen et al. 2017). California's water resources provide not only drinking water but also water for irrigation and wetland maintenance. The California water supply is broken into many uses throughout the state, with over 40% going to agricultural irrigation and a small percentage going to urban water for personal use as seen in Figure 6 (Allen et al. 2017). This would seem to indicate irrigated agriculture is the "low hanging fruit" to research water conservation for the State of California. Previous water saving initiatives, in response to earlier droughts, had focused on constricting residential water use. This effort effectively reduced water waste for California residents. However, with most of urban water utilized for land irrigation, further constrictions in residential water use would not produce the desired outcome of reducing water use while meeting the Governor's urban water conservation targets. This project explores how to meet that 20% reduction of urban water use through a comparison of evapotranspiration models and methodologies for irrigated lands.

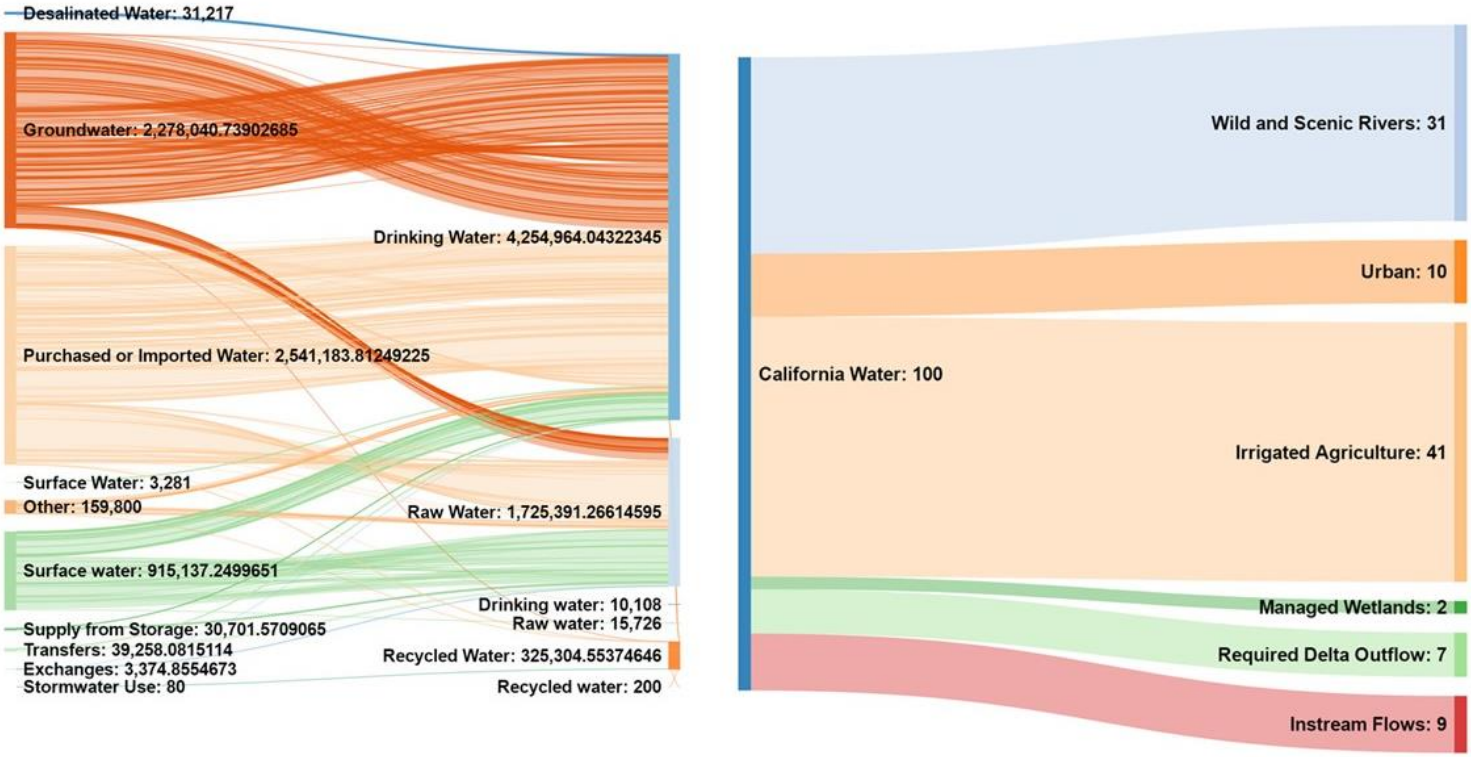

Figure 6 Quantified 2015 urban water flow nodes and water use in California (Source: Allen et al. 2017)

1.2 Evapotranspiration

There are two different measures of evapotranspiration: Potential Evapotranspiration (PE) and Actual Evaporation (AE). Potential Evapotranspiration (PE) measures how effective the atmosphere removes water from the surface using evaporation and transpiration with an unlimited water supply (Pidwirny 2006). PE is an energy-driven process, with the majority (80%) of it coming from the sun. Wind is the second factor as wind removes water from the ground to the atmosphere by a process called eddy diffusion (Pidwirny 2006). In addition, the gradient of vapor pressure plays a major role in accelerating the evapotranspiration rate (Pidwirny 2006). These two measures are then used to calculate how much water the crops need. Actual Evaporation is the water that is removed from the effects of evaporation and transpiration (Pidwirny 2006). California is a semi-arid region which makes it critical every drop of water is being used in the most efficient

manner possible. Comprehending how much water is needed, can save hundreds of thousands of gallons of water if properly calculated. An ET of 25.4 mm or one inch means the farmer needs to irrigate with 27,154 gallons to replace the water lost to the evapotranspiration.

As an example, say that a farmer mistakenly overestimated and calculated his reference ET, the water lost from land surfaces, stomata, and vegetation, as 0.5 inch for that day when it was only 0.35 inch. That means the farmer will irrigate the crops with wasted extra gallons of water. Not only is that urban water waste but, it could mean an overwatering of the field, flooding of new seedlings, washing away of topsoil, and ruination of the crop.

1.2.1 Evaporation Model – Penman Monteith

This method is a weather-based methodology for calculating reference evaporation. It uses data from ground-based weather stations as input to calculate the Penman-Monteith equation. The Penman-Monteith model is the most commonly used method for computing irrigation needs for crops and other surfaces that require irrigation (Cai et al. 2007). This method will be discussed in greater detail in chapter 2.

1.2.2 Evaporation Model – NDVI Triangle

The NDVI Triangle method for calculating evapotranspiration is based on multispectral and thermal imagery bands from the LDCM orbiting satellite. This technique is relatively new and, according to my research, has not been used in southern California, to calculate evapotranspiration for a large area. The use of satellites instead of ground-based stations brings flexibility to the estimation of evapotranspiration. This methodology is discussed in greater detail in chapter 2 as well.

1.3 Study Area

The Moulton Niguel Water District (MNWD), shown in Figure 7, was selected as

the study area for this project as its service area covers my own residence and the residences of family and friends. The MNWD provides water, recycled water and waste water treatment to approximately 170,000 southern California customers that live in Aliso Viejo, Laguna Niguel, Laguna Hills, Mission Viejo, Dana Point, and San Juan Capistrano (Moulton Niguel Water District, 2017).

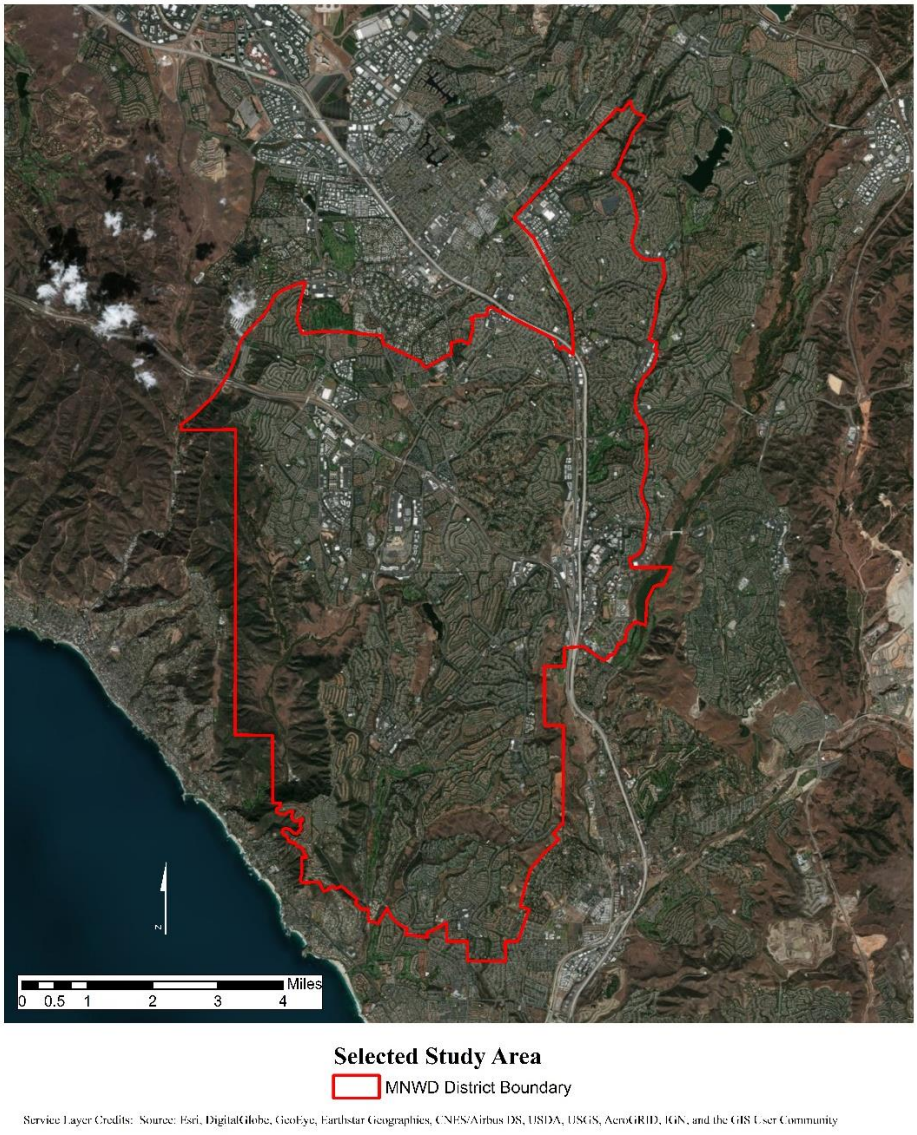

Figure 7 MNWD study area selected for evapotranspiration comparative study (Source: California Data Collaborative / CA-Stormwater-Data-Challenge)

Weather station #245, the basis of the ground-based ET measurement, lies four miles to the east of the (MNWD) service area. This weather station was selected as it was the closest working weather station with obtainable historical data for this study period and, in addition despite the distance, the land, soil, and climate, is like that of the MNWD. CIMIS station #245 is situated on the Coto de Caza Golf & Racquet Club greens, centered in the north most fairways on top of well irrigated and maintained turf grass at a latitude of 33º37'18N & longitude 117º35'7W. CIMIS Station # 245 collects data hourly on a minute-by-minute basis. This station uses the Penman-Monteith equation to calculate reference ET. The assumption for the reference crop, for the Penman-Monteith equation, is a height is 0.12m with a fixed surface resistant of 70 sm-1 and an albedo value of 0.23 (Zotarelli et al. 2009).

The water needs of Orange County have increased with the population growth in urban areas. The population of Orange County, California grew from 3,010,232 residents in 2010 to 3,172,532 in 2016 (TIGERweb 2017). More residents mean more water consumption. As water supplies are limited, initiatives to conserve urban water across the county may be promoted. In 2016, the Metropolitan Water District (MWD) provided drinking water to nearly 19 million people in parts of Los Angeles, Orange, San Diego, Riverside, San Bernardino, and Ventura counties, and delivered an average of 1.7 billion gallons of water per day to a 5,200-square-mile service area (Lopez 2017). The MWD is the largest distributor of treated drinking water in the United States. Water provided by MWD is imported from Northern California via the State Water Project and the Colorado River via the Colorado River Aqueduct. MWD infrastructure also includes 16 hydroelectric facilities, nine reservoirs, 819 miles of large-scale piping, and five water treatment plants (Allen et al. 2017). The Municipal Water District of Orange County (MWDOC 2017), a wholesale importer of water from MWD, treats the water at the Diemer Filtration Plant in Yorba

Linda and delivers the treated water to its customers through the East Orange County Feeder #2 and the Allen-McColloch Pipeline ("Request for Proposal Water/Recycled Water/Wastewater Cost of Service and Rate Design Study" 2017). That water is then supplied to the MNWD for dissemination to the residents of the service area (Allen et al. 2017).

1.4 Research Objectives

This study measured evapotranspiration using two different methods and sought to investigate the following three research objectives:

- To assess the effectiveness of estimating ET using ground and satellite-based methods;
- To determine the correlations between ground and satellite-based methods of calculating ET; and
- To determine the practicality of using a satellite-based method of measuring ET with considerations to the required software availability, necessary GIS operator skill level, and number of available personnel able to master the techniques needed for this method.

1.5 Thesis Organization

Chapter 2 discusses Evapotranspiration in greater detail and examines past work calculating Reference evapotranspiration using the traditional method and the Triangle Method which uses satellite imagery. Chapter 3 provides the many calculations and methods needed to obtain reference Evapotranspiration for both the Penman-Monteith and NDVI Triangle method. Chapter 4 presents the results obtained using the two methods and discusses why one model may be more appropriate than the other. Chapter 5 offers some conclusions and suggestions for future work.

Chapter 2 Related Work

Evapotranspiration is the critical value, which tells growers when to water and irrigate, when to stop, and when to adjust the irrigation flow as the climate changes. There are a variety of ways to calculate reference evapotranspiration, but none is more globally used than the Penman-Monteith model (Liang et al. 2012). This model is used by the 145 CIMIS weather stations to calculate Evapotranspiration using ground-based sensor data as input as seen in Figure 8. This study sought to determine if the Triangle method can be reliably used as a substitute for the Penman-Monteith method to measure evapotranspiration.

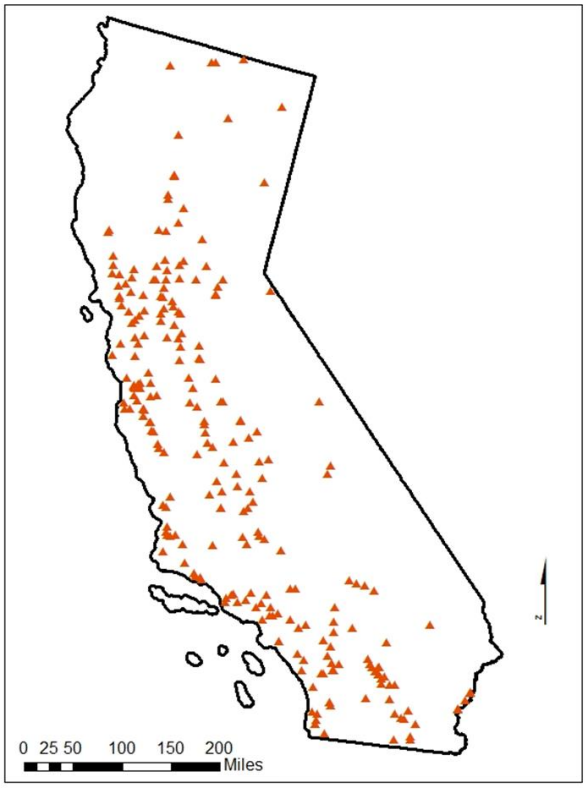

Figure 8 CIMIS weather stations in California
Source: http://www.cimis.water.ca.gov/.

2.1 Water Conservation Efforts in California

Since much of California is an arid to semi-arid state and the necessity to conserve water is quite high, many different methods have been employed with varying degrees of success. Ward and Pulido-Velazquez (2008) noted, during their studies of water conservation efforts, the use of subsidies was unlikely to create any improvement in the overuse of water resources. Dickerson et al. (1992) used the psychological method of Cognitive Dissonance to Encourage Water Conservation. This approach tried to shame people from abusing and wasting water resources after being reminded of past behavior. The heart of the study was the public commitment the participants took not to waste water as it created a sort of "hypocrisy condition" for the participants. The method worked, however, only on those that were exposed to the hypocrisy conditioning. Ferguson (1987) observed that methods to conserve water of irrigate agriculture fields could not be used and applied to urban residential landscapes, without amendments. Allen et al. (2005) noted, California and the west coast has a unique hydrogeological structure. By observing only small amounts of deep percolation, which leaves the project directly for subsurface flows, it is conducive for very accurate measurements of evapotranspiration. After measuring the limited benefits of using subsidies to promote urban water savings, Ward and Pulido-Velazquez (2008) concluded that a more structured and scientific way to measure and conserve water was needed for California. Monteith (1965) used evapotranspiration to explain the movement of water, evaporation, from soil and land surfaces. In addition, the transpiration from the surfaces and stomata of plants were also included in his calculations. He combined the all the factors that caused transpiration from plants and evaporation from the ground surfaces and formed relationships. He connected the rates of evaporation with heat exchange and created, along with his partner Howard

Penman, a formula to determine a reference evapotranspiration model. This model was called the Penman-Monteith model.

2.2 Penman-Monteith Reference Evapotranspiration Model

The Penman-Monteith Reference Evapotranspiration Model is the most widely used and highly regarded standard for measuring reference evapotranspiration (Liang et al. 2012). This model was developed over 50 years ago and has been continuously refined to estimate evapotranspiration, accurately, for different climates (Zotarelli et al. 2009; Allen et al. 1998). There was a need to standardize the measurement to better accommodate the users and their availability to weather data. After a test of four different evapotranspiration models (the Blaney-Criddle, radiation, modified Penman, and pan evaporation) to establish which method best met the guidelines as published in the FAO Irrigation and Drainage Paper No. 24 'Crop water requirements (1998), The Penman – Monteith equation was considered superior with the best results and lowest error for a living grass crop (Allen et al. 1998).

However, due to the large number and variety of inputs required from CIMIS weather stations, it is not a practical method for many areas. The California Irrigation Management Information Systems (CIMIS) weather stations measure air temperature, relative humidity, precipitation, solar radiation, wind direction, and wind speed amongst other weather data. These are all utilized to calculate ET, for the Penman-Monteith equation as well as a modified version of the Penman-Monteith equation. Statistically, however, there is not a difference between the two Penman-Monteith methods (Temesgen et al. 2018).

The Penman-Monteith equation requires the inputs listed in Table 1. However, many locations cannot afford to calculate the reference ET values to collect these input data. Other ways to collect these inputs, such as satellite imagery, must be considered as viable solutions.

Table 1 Summary of data needs for Penman-Monteith Method

#	Name	Source	Format	Purpose
1	Mean daily temperature	Station #245	Collected/calculated value	Used to calculate T_{mean} which is a feeder equation for four calculations for Penman-Monteith
2	Mean daily solar data	Station #245	Collected/calculated value	Measures the strength of solar radiation
3	Wind Speed	Station #245	Collected/calculated value	Measured for evaporation effect
4	Slope of saturation vapor pressure curve	Calculated T_{mean}	Collected/calculated value	Find relationship of saturation vapor pressure and temperature
5	Atmospheric Pressure	Station #245 MSL	Collected/calculated value	Pressure from Earth's atmosphere as it affects ET
6	Psychrometric constant	Station #245	Collected/calculated value	Relates partial pressure of water in the air to the temperature vapor pressure est.
7	Delta Term (DT)	Slope of saturation, wind speed, psychrometric constant	Collected/calculated value	Used to calculate the radiation term for the overall reference ET equation
8	Psi Term (PT)	Slope of saturation, wind speed, psychrometric constant	Collected/calculated value	Used to calculate the Wind Term of the overall reference ET equation
9	Temperature Term (TT)	Station #245/ Weather Underground	Collected/calculated value	Used to calculate the Wind Term of the overall reference ET equation
10	Mean saturation vapor pressure	Station #245/ Weather Underground	Collected/calculated value	Used to calculate saturation vapor pressure from air temperature

	derived from air temperature(es)			
11	Maximum daily temperature at 2 m height, °C	Station #245	Collected/calculated value	Used to calculate the mean saturation vapor pressure
12	Minimum daily temperature at 2 m height, °C	Station #245	Collected/calculated value	Used to calculate the mean saturation vapor pressure
13	Actual vapor pressure (ea) derived from relative humidity	Station #245/ Weather Underground	Collected/calculated value	Used to calculate actual vapor pressure from relative humidity
14	The inverse relative distance Earth-Sun (dr) and solar declination (δ)	Julian date	Collected/calculated value	Used to calculate the sunset hour angle
15	Conversion of latitude (φ) in degrees to radians	Latitude conversion of study area	Collected/calculated value	Converts the latitude of the study area to radian for use in the Penman Monteith equation
16	Extraterrestrial radiation (Ra)	Solar constant, solar dec. and time of year	Collected/calculated value	Calculates the intensity of solar radiation based upon the angle of the sun
17	Clear sky solar radiation (Rso)	MSL and the calculated Ra	Collected/calculated value	Used to calculate net longwave radiation
18	Net solar or net shortwave radiation (Rns)	Mean daily solar radiation calculation albedo constant	Collected/calculated value	Used to calculate the cloudiness of the sky
19	Net outgoing long wave solar radiation (Rnl)	T_{min}, $T_{max,}$ The Stefan – Boltzmann constant, calculated actual vapor	Collected/calculated value	Used to measure the Earth's emission of radiation

		pressure, calculated incoming and clear sky radiation		
20	Net radiation (Rn)	Shortwave and longwave radiation	Collected/calculated value	Used to calculate the difference between the long and short-wave radiation

Cai et al. (2007) says of all the values that are needed to calculate ET using the Penman-Monteith method, most are not available, and weather stations that could collect these data are very expensive, and not affordable for most areas. Davis and Dukes (2012) counter that argument as they used, in a study with the southern California MWD, affordable ET controllers to control irrigation through ET calculations for three types of landscapes: cool season turf on loam soils with full sun, shaded annuals on sandy soils, and low water using ground cover on a sunny, 20° slope. The tests showed there was very little over irrigation. Due to general and broad settings on the controller, however, there were many water deficits throughout the testing period which resulted in areas with insufficient irrigation.

The Penman-Monteith method performs well in areas with arid or humid climates. Tegos et al. (2015) tells us that the detailed measurements that are required for this method are dependent upon the number of weather stations that are available. Without the density of stations, especially in sparsely populated places, the evapotranspiration values become unreliable (Tegos et al. 2015). The Penman-Monteith model, which is a ground-based system, is susceptible to errors. Westerhoff (2015) points out the uncertainty that comes with the input equations. He discovered the reference ET as measured by the Penman-Monteith ground source method, is most sensitive to temperature,

solar radiation, relative humidity, and the cloudiness ratio, and that errors may range from 10 to 40 percent.

2.3 Triangle Method Model

Satellite imagery that show differences in land cover, harvested crop lands, lands used by grazing cattle and irrigated crops and waterbodies are indicators of possible patterns for ET (Schmugge et al. 2002). Lillesand, Kiefer and Chipman (2012) point out, with high-resolution cameras, vegetation and land cover conditions can be seen, gathered and transmitted from orbiting instruments for critical analysis of ET. Using their data to determine the wet and dry edge of the triangle when surface temperature and NDVI are combined in a two-dimensional plot, reference evapotranspiration can be estimated. The Triangle method requires satellite input, the ability to calculate multispectral and thermal bands and develop two-dimensional maps to estimate evapotranspiration between the dry and wet edge (Suzuki et al. 2004).

2.3.1 Triangle Method Workflow

The workflow of data gathering was mapped so that a repeatable process could be used for a repetitive process. Some of the difficulties included creating band math from equations, creating a Region of Interest (ROI) within the thermal bands, and matching map future resolutions with previously created data sets. Each calculation, much like the Penman-Monteith formula, builds upon each other and becomes the input for the next equation as seen in Figure 8. These steps will be explained in more detail in Chapter 3.

The Triangle method is a way to calculate, using remotely sensed data, evapotranspiration values through two-dimensional NDVI pixel plots, regardless of geographic location. Suzuki and Masuda (2004) noted that NDVI is a reasonable measure of ET in a large- scale area. For this project, a region of interest was created in ENVI to reflect the MNWD. NDVI can give a value

equal to traditionally measured ET (Suzuki et al. 2004). The triangle method is a comparison of NDVI and Land Surface Temperature (LST), in °C, to determine wet and dry edges of the measured surface. The top of the triangle is the lowest Evaporation as it represents bare earth as the bottom of the triangle is representative of maximum ET. These two values are plotted as X/Y values to create a measure of evapotranspiration. Suzuki and Masuda (2004) observed that NDVI, obtained via remote sensing, has equivalency to evapotranspiration measured in more traditional ways while Cai et al. (2007) argues the weather-based Penman-Monteith method has provided consistent ET values over a variety of regions and climates.

The calculation of the NDVI Triangle starts with the Surface Energy Balance Algorithm for Land (SEBAL). SEBAL estimates evapotranspiration, spatially, using energy balance, satellite imagery, and spectral analysis (Bastiaanssen et al. 1998). With this method, Vegetation indexes, Land Surface Temperatures, and evapotranspiration can be calculated for a region. SEBAL can be used without knowledge of the ground being measured, independent of ground-based weather stations. This makes it especially useful in remote areas.

To use the satellite imagery, the normal mathematical computations for the vegetation indexes and surface temperatures must be put into a format that can be understood and visualized geographically. The way to accomplish this is to use band math. Band math converts the static measure of an equation and uses band math to convert the imagery to that equation. For example, the NDVI equation is Near Infrared (NIR) – Red divided by Near Infrared (NIR) plus Red. Band math associates that measurement to the sensors on a satellite that measures NIR and Red and completes that equation and produces a two-dimensional scatter plot based upon the pixels gathered from the satellite image. The spectral data can be compared to spatial location to gain insight on a Region of Interest.

2.4 Penman-Monteith Model vs Triangle Method

The results of using the NDVI Triangle method were compared with the results obtained with the Penman-Monteith method using the methods of Suleiman and Hoogenboom (2007) to analyze statistical error and determine model performance for the MNWD.

Triangle method relies on wet and dry edges to determine the Evapotranspiration when compared to the calculated surface temperature from the LDCM (Suzuki et al. 2004; Bastiaanssen et al. 1998).

The Penman-Monteith has proven to be effective measures of reference of evapotranspiration in the climate that fits the strength of its equation. Beyazgül, Kayam and Engelsman (2000) states the Penman-Monteith method performed excellently in both humid and arid climates. However, The Penman-Monteith model tends to overestimate in hotter climates (Tegus, Alamos and Houstonians 2015; Pandey et al. 2014; Jhajharia, DebBar and Argrawal 2004).

Suleiman and Hoogenboom (2007) used the Penman-Monteith evaporation method for the humid climate of Georgia, for daily reference evapotranspiration estimation. This study was done as a comparative study between the Penman-Monteith and Triangle method of calculating evapotranspiration. They found that in a humid climate the Penman-Monteith equation yielded a more accurate value for reference evapotranspiration than the Triangle Method. They set up the study using nine sites with weather stations. These weather stations, part of a larger collection of 70, collected weather data for agriculture, including irrigation and water management. The Penman-Monteith requires many climatic inputs and, those inputs were gathered from the nine chosen weather stations for this study. The weather stations provided, air temperature, relative humidity, precipitation, wind speed, wind direction, solar radiation, soil moisture, soil temperature, and barometric pressure. These are all the inputs needed to calculate a reference evapotranspiration.

From that gathered data, calculations for the Penman-Monteith equation were conducted. Quality control checks were performed daily, and the research team reported no missing data for this study from the nine sensors. The Triangle method requires multispectral and thermal sensor inputs and the proper program to calculate and display two-dimensional plots to visualize the estimated evapotranspiration between the dry and wet edge (Suzuki et al. 2004).

This project followed Suleiman and Hoogenboom (2007) method of data collection from Station # 245 (Coto de Caza) and used the collected weather values to calculate reference evapotranspiration for the Penman-Monteith method. The Triangle model, for this study, used the Surface Energy Balance Algorithm for Land (SEBAL) to estimate evapotranspiration through the calculation of essential hydro-metrological parameters (Bastiaanssen et al. 1998).

Chapter 3 Methodology

The aims of this thesis were to: 1) assess the effectiveness of estimating ET using ground and satellite-based methods; 2) determine the correlations between ground and satellite-based methods of calculating ET; and 3) determine the practicality of using a satellite-based method of measuring ET with considerations to the required software availability, necessary GIS operator skill level, and number of available personnel able to master the techniques needed for this method.

The weather-based Penman-Monteith method uses multiple weather data measurements as primary input to estimate ET. Data can be obtained from CIMIS online data portal. Alternatively, the NDVI Triangle method uses satellite imagery from the LDCM as the primary data input to estimate ET. Data need to be manipulated before use in evapotranspiration measurements. The intent is to discover, using statistical analysis, if the NDVI Triangle method might provide a suitable alternative to the Penman-Monteith method for locations that lack weather stations.

3.1 Research Design

This project involved the calculation of evapotranspiration on four different days in 2016 using ground-based weather stations and orbiting satellites. The spatial differences between the CIMIS weather station # 245 located on the Coto De Caza golf course and the area of study, the MNWD located four miles to the west is negligible because the two locations share similar soil types, climates, and humidity. ENVI 5.4, ENVI Classic, LDCM at 30 m for multispectral, and 100 m but resampled to 30 m pixels for thermal bands, excel for computations, ArcGIS and ArcMap were the main tools and data used for this project.

3.2 Penman-Monteith Evapotranspiration Model

The Equation 1 shows the Penman-Monteith formula for calculating ET Reference for clipped grass reference crop. This formula assumes the hypothetical crop has a height of 0.12 m, a

fixed surface resistance of 70 s m^{-1} and an albedo value of 0.23. The albedo measure is the portion of light reflected off the surfaces of leaves (Zotarelli et al. 2009). This equation reads as:

$$ETo = \frac{0.408\Delta\,(R_{n-G}) + \gamma \frac{900}{T+273} u_2 (e_s - e_a)}{\Delta + \gamma(1 + 0.34\,u_2} \quad (1)$$

Where:

ET_o is the reference evapotranspiration in mm day^{-1};

R_n is the net radiation at the crop surface in MJ m^{-2} day^{-1};

G is the soil heat flux density in MJ m^{-2} day^{-1};

T is the air temperature at 2 m height in °C;

u_2 is the wind speed at 2 m height in m s^{-1};

e_s is the saturation vapor pressure in kPa;

e_a is the actual vapor pressure in kPa;

e_s - e_a is the saturation vapor pressure deficit in kPa;

Δ is the slope vapor pressure curve in kPa $°C^{-1}$;

γ is the psychrometric constant in kPa $°C^{-1}$.

Weather sensors contribute greatly to the calculation of evapotranspiration as the Penman-Monteith formula requires several different climate inputs.

3.2.1 CIMIS Sensor

As indicated in the Penman-Monteith equation and Table 1 in chapter two, there are many inputs required to calculate evapotranspiration. For this study area, the Moulton Niguel Water District (MNWD) weather sensors, maintained by CIMIS, gather and collect data needed to calculate evapotranspiration for the area on a minute-by-minute basis. The weather sensor used for this project study is located at an elevation of 846ft Mean Sea Level (MSL). Sensor #245 is

centered on the northernmost fairway, placed amongst several acres of irrigated and maintained turf grass as seen in figure 9 (Temesgen et al. 2018).

Figure 9 Coto De Caza CIMIS weather sensor #245
(Source: Temesgen et al. 2018; https://eros.usgs.gov//)

A concern for this sensor is that the sand traps and nearby houses, depending on the wind direction, may compromise the data collected. This is because obstructing buildings can either cut down on wind exposure to the collecting sensor or redirect the wind. H Jiang (2014) observed sand traps disturbed the velocity field and the wind-sand coupling effect can greatly change the wind flow field.

The data needs to calculate the Penman-Monteith formula are listed in Table One. The data and evapotranspiration values were taken directly from the sensor database itself. The Penman-Monteith calculations were done via the weather station internal sensors.

3.2.2 Sensor Data Collection

The CIMIS weather station collects a variety of environmental data. As evapotranspiration is affected by many weather and climate factors, one sensor needs to measure many readings, in one location, for consistency.

3.2.2.1 Total Solar Radiation

Sensor #245 used a pyranometer, which is a collection of thermocouples that generate electricity according to how much solar radiation is received. Woodford (2017) better explains this relationship, the more sun, the hotter the temperature gets, the more electricity the pyranometer produces. The response varies with the angle of the sun: when the sun is directly overhead, the maximum electricity is generated. The greater the angle of the sun changes, the less electricity is produced. When the sun starts to move from its 12:00 noon position, the CIMIS sensor performs a cosine correction to adjust for the change of electrical changes due to angle difference (Temesgen et al. 2018). However, the measured radiation was measured in Langley units instead of Mega joules; Mega joules is needed for the Penman-Monteith Equation.

3.2.2.2 Soil Temperature

This sensor uses a negative temperature coefficient thermistor, which is a temperature-resistant resistor whose resistance decreases as the temperature rises. This sensor measures soil temperature in °C. This project used negative temperature coefficient thermistors to indicate if electrical equipment was overheating. For this study, this is an important piece of data as it is a major part of evaporation. The more sun hits the ground, the more the soil heats up. When the soil heats up, evaporation starts to increase.

3.2.2.3 Air Temperature / Relative Humidity

This sensor also uses a thermistor to measure air temperature. This is a primary feed in to the calculation as the temperature maximum and minimum values are used to calculate the average temperature which is then used to estimate the Temperature Term (TT), which is used to calculate the Wind Term for the overall Penman-Monteith equation, minimum daily temperature, actual vapor pressure, and net outgoing long wave solar radiation for the Penman-Monteith formula (Temesgen et al. 2018).

The same sensor also measures humidity using a combination of wet and dry bulbs. The humidity of the atmosphere is measured in percent. Anderson (1936) recognized that percent humidity, by itself, is not strictly a measure of dryness but the vapor pressure deficit. This measurement requires the input of partial pressure in the air as compared to the air temperature using paired wet and dry thermometers. The psychrometric stays constant and an average atmosphere condition was used for this computation. Loescher et al. (2009) however, disagree with the psychrometric being labeled a constant. They recommend using open- and-closed-path infrared gas analyzers (IRGAs) because these instruments operate at greater than 10 megahertz, which is the speed at which latent energy flux is transported (Loescher et al. 2009).

3.2.2.4 Wind Direction / Wind Speed

The Penman-Monteith method requires wind direction and speed measured two m above the ground. The direction was measured with a wind vane and the wind speed was measured with an anemometer, a device that simply turns as fast as the wind is blowing. The concern for station #245 is the fact sand traps and houses lie near the weather sensor. These two obstacles can affect the quality of wind readings (Temesgen et al. 2018).

3.2.2.5 Slope of Saturation Vapor Pressure Curve (Δ)

When an equilibrium is reached between water molecules escaping and returning to the water reservoir, the air is said to be saturated since it cannot store any extra water molecules. The associated pressure is called the saturation vapor pressure (Manivanan 2006).

The higher the air temperature, the more water molecules can be stored. Consequently, the higher the storage capacity, the higher its saturation vapor pressure (Manivanan 2006). I calculated this value by using the Tmean calculated in section 3.2.1 and the constant for the base of the natural logarithm (i.e. 2.7183).

3.2.2.6 Atmospheric Pressure (P)

The atmospheric pressure is the pressure exerted by the weight of the Earth's atmosphere. The higher the altitude, the more evapotranspiration is promoted due to low pressure (Zotarelli et al. 2009). For this equation this project found and plugged in the Mean Sea Level (MSL) elevation of the Coto de Caza weather station # 245.

3.2.2.7 Mean Saturation Vapor Pressure

As discussed, the slope of saturation vapor pressure curve, is related to air temperature. (Manivanan 2006) This project accomplished the calculation of the mean saturation vapor pressure curve by calculating the mean between the saturation pressure at both the minimum and maximum

temperature. From that point, the mean saturation vapor pressure was calculated, from the daily minimum and maximum temperatures.

3.2.2.8 Actual Vapor Pressure (ea)

Relative humidity was used to calculate actual vapor pressure for this equation. Anderson (1936) recognized that percent humidity, by itself, is not strictly a measure of dryness but the vapor pressure deficit.

The calculation of the variables for the Penman-Monteith methodology are all completed on-site via the collecting weather station: Weather station #245 collects and calculates evapotranspiration. In addition, the data used to calculate ET is available for review and analysis. The measured data includes solar radiation, air temperature, soil temperature, relative humidity, wind speed, wind direction, and precipitation. The calculated values that are available through the CIMIS station are net radiation, reference evapotranspiration, wind speed and direction, wind run, vapor pressure, and dew point temperature (Temesgen et al. 2018). The reports available for each reporting station are hourly, daily, and monthly reports, daily ETo variance reports, and monthly average ETo reports. This data, accessible through the CIMIS website, is downloadable in four formats: Web, XML, CSV, and PDF.

3.3 NDVI Triangle Method

The triangle method is a way, using remotely sensed data, to calculate evapotranspiration. Suzuki and Masuda (2004) noted that NDVI is a reasonable measure of ET in large areas. For this project, a region of interest was created to reflect the MNWD area. NDVI, when compared to surface temperature, can give a value equal to traditionally measured ET (Suzuki et al. 2004). The triangle method is a comparison of NDVI and LST to determine wet and dry edges of the measured surface. The top of the triangle is the lowest Evaporation as it represents bare earth as the bottom of the

triangle is representative of maximum ET. This seen in Figure 10. ENVI permits the manipulation of data to a point you can select areas of the triangle and associate it with the map as far as determining the location of the highest and lowest ET as seen in Figure 11. This image visualizes the Arroyo Trabuco golf course, Casta del Sol golf course, Lake Mission Viejo, and the Sulphur Creek Reservoir as areas of high ET. Figure 10 also classifies the wet/dry edge.

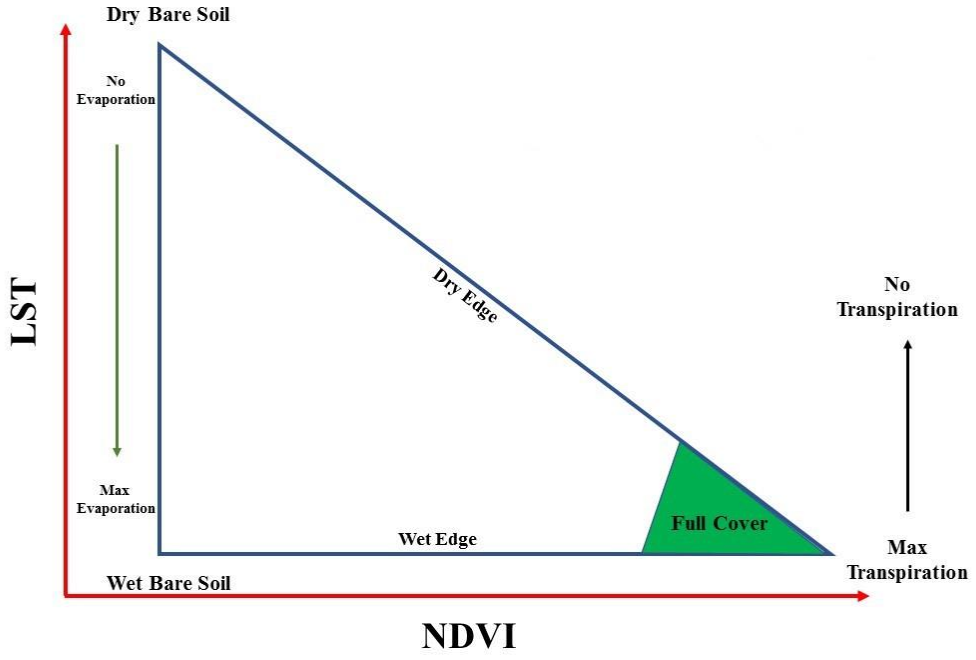

Figure 10 Calculation of estimated evapotranspiration by NDVI in triangular space (Source: Han et al. 2004)

The red areas indicate the dry edge or areas of low ET. That is representative of areas that are residential, roads, or dirt. Water absorbs light, so satellite imagery will read those areas as a dark color such as blue or black. Those would be areas of high evapotranspiration potential. Inversely vegetation will appear as green due to its low reflective and high absorptive nature of red and infrared due to the chlorophyll in plants. Bare earth, dirt and areas with low vegetation coverage

will more easily reflect Red and will indicate as such when viewed through the multispectral bands of a satellite (GISGeography 2018).

3.3.1 Data Collection

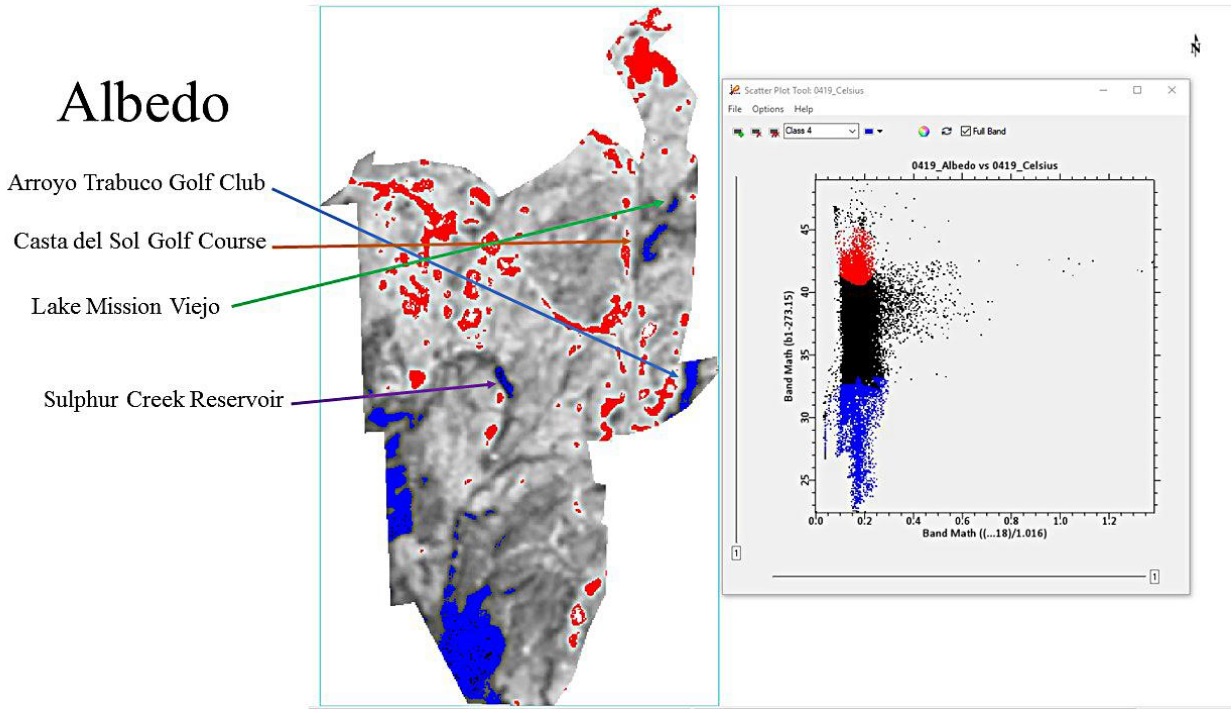

Figure 11 Identification of areas of potential high ET by the use of albedo in the MNWD study area (Source: https://earthexplorer.usgs.gov/)

The NDVI triangle methodology requires the application and manipulation of remotely sensed data for calculation of the triangle. This method requires the most skill as the data is created by the user through Region of Interest (ROI) designation, band selection, and spectral analysis of the GeoTIFF elected, after determining the requirements for the study area as seen in Figure 10. The triangle method eliminates the need for base-station input as all data is collected from the orbiting body. ENVI proved to be the program of choice as it was found to be the most applicable for the project's satellite imagery processing needs. This program provided the ability to more accurately determine and visualize NDVI Triangle values.

For this project, the LDCM was selected instead of MODIS data. The main advantage of MODIS is more frequent passes. This would have allowed the use of all 20 days for this project study. On the other hand, the disadvantage of MODIS, is the coarse resolution. The main advantage of the LDCM satellite is (a) very good resolution, 30 m at multispectral and 30 m at thermal. The disadvantage is, the pass is only every 16 days. This caused some difficulty when attempting to line up specific days to measure. Considering the temporal limitation of LANDSAT, four days, as recorded by the LDCM for this project were matched out of the 20 days in 2016 (08 February, 19 April, 22 June, and 08 July). To ensure directed and purposeful readings, a Region of Interest (ROI) was created in ENVI of the Moulton Niguel Water District (MNWD). A mask was generated for that ROI, so calculations could only read what is inside the ROI and nothing outside of it. The intercept, slope, and the coefficient of determination was calculated for all four days. The temperature was then converted from K to °C from the LDCM's thermal bands.

3.3.2 Workflow

A summary description of the workflow used to calculate the NDVI Triangle for the MNWD is shown in Figure 12. The data Source for the NDVI Triangle method is the LDCM OLI/TIRS C1 Level-1 Multispectral (30 m) data/7 BSQ through USGS earth explorer and the program used to construct the triangle was: Environment for Visualizing Images (ENVI).

Figure 12 NDVI Data processing required for NDVI Triangle method.

Multiple computations were completed to identify NDVI, ALBEDO, SAVI, WDVI, L Value, via band math as seen in Appendix A. In addition to band math, band layering highlighted characteristics of the area to identify foliage growth of varying conditions. To that end NDVI and LST were calculated and combined, using the SEBAL method, to estimate evapotranspiration values for the Moulton Niguel Water District.

3.4 Statistical Analysis

To measure performance of the Penman-Monteith and the remotely-sensed NDVI Triangle evapotranspiration model, statistical analysis was needed. Equation 2 shows the Root Mean Square Error (RMSE) which measured how far from the regression line the data falls. The lower the

RMSE value, the better the agreement (Suleiman et al. 2007). Equation 3 shows the index of agreement (d), which measured the predicted error. This varies between -1.0 and 1.0. A value of 1.0 means a perfect agreement while a value a value of 0 would indicated a poor one (Willmott et al. 2011). The Root Mean Square Error (RMSE) and the index of agreement (d) was used to determine the value for agreement between the two models. Willmott, Robeson and Matsuura (2011) tells us these two calculations are useful in calculating the performance of diverse models. Equation 4 shows the Mean Absolute Deviation (MAD). This equation was selected because, as a performance measure, it is not overly sensitive to outliers. Equation 5, the Mean Absolute Percentage Error (MAPE) formula was used to determine trend analysis and the forecasted error of measurement.

$$RMSE = [N^{-1} \sum_{i-1}^{N} (P_{i-} O_i)^2]^{0.5} \quad (2)$$

Where:

N is the number of cases

O is the observed

P is the predicted ET

$$d = 1 - [\frac{\sum_{i-1}^{N} (P_{i-} O_i)^2}{\sum_{i-1}^{N} (|P_i|_- |O_i|)^2]} \; 0 \leq d \leq 1 \quad (3)$$

Where:

d is the index of agreement

O is the observed

P is the predicted ET

$$MAD = \frac{1}{n} \sum_{i=1}^{n} | x_{i-} \bar{x}| \quad (4)$$

Where:

n is the number in the data set

i is the percentile location

$$MAPE = \frac{\sum_{t=1}^{n} |(A_t - F_{t/A_t}|}{n} \quad (5)$$

Where:

A is the actual value

F is the predicted value

Chapter 4 Results

The use of satellites and remote sensing to measure evapotranspiration provides viable options to areas that find the acquisition, maintenance, and repair of more expensive weather monitoring stations beyond their ability to obtain and sustain. Remote sensing to measure evapotranspiration provides global versatility to the scientist and removes the geographic limitations one would have with an earth-bound measuring point. Ground-based weather stations are limited to a single form of measurement as it is dictated by the installed hardware. In contrast, there are many satellites that measure an array of readings depending on the need of the user and the mission of the remote body. The ability to compare remote sensed readings of one satellite against another provides a better comparative analysis when you can access a multitude of differently obtained data for the same study area.

The objectives for this study were to assess the effectiveness of estimating ET using ground and satellite-based methods, determine the correlations between ground and satellite-based methods of calculating ET and, determine the practicality of using a satellite-based method of measuring ET with considerations to the required software availability, necessary GIS operator skill level, and number of available personnel able to master the techniques needed for this method. For this study the LDCM satellite data was used to calculate estimated evapotranspiration in the MNWD by NDVI in triangular space. The results of data gathering, and final calculations are presented in Tables 5 and 6. The visual analysis for the Triangle Method is presented in Figure 13. The two-dimensional pixel scatter plots for the Triangle method for the days of 08 February, 19 April, 22 June, and 08 July 2016 were formed from the mathematical computation of the LDCM's multispectral bands and thermal bands. The Land Surface Temperature (LST) is represented by the

Y axis while the X axis shows the NDVI computation. When compared together, they create a two-dimension pixel scatter plot in triangular space.

4.1 Penman-Monteith Method Results

The evapotranspiration calculation was performed by using the Penman-Monteith method with data collected with station # 245. This calculation was performed internally by the station itself and was determined to be suitable for the MNWD due to the similarity of the landscape and climate of the area. This calculation was used as the base comparison to determine the accuracy of the NDVI Triangle method. The reference data and evapotranspiration estimates for the 08 February, 19 April, 22 June, and 08 Jul 2016 are summarized in Table 3. These data points were collected at 12:00 p.m. on cloudless sunny days to estimate maximum evaporation and transpiration potential for the days of measurement.

All the calculations for evapotranspiration were performed on-site, within the weather station itself. The findings were uploaded to CIMIS, a minute-by-minute basis, to match the frequency of data collection. This frequency allows the grower and irrigator to quickly pivot and adjust water irrigation based on yesterday's readings. The Triangle method, though versatile in an area of measurement, cannot meet those operational standards.

The data collected by this weather station is accurate for the surrounding area. Weather station # 245 data readings can be influenced by external interferences. Wind is the second biggest factor, after the sun, for evaporation and transpiration processes However, the average wind speed for the entire year of 2016 at weather station #245 never exceeded 1.7 m/s (Temesgen et al. 2018). Another factor that may affect ET readings is the fact that the current location, situated on well-watered and irrigated blue grass, may affect the soil temperature readings which in turn reflect in the evapotranspiration readings. These readings may not reflect the expanse land of which these

readings represent. The soil temperatures predictably waxed and waned with the changing of the seasons, with a high of 21.3 °C in July 2016 and a low of 11.8 °C in January (Temesgen et al. 2018). Each of the weather station's sensors must be calibrated as they are exposed to the elements and inclement weather. As the Penman-Monteith requires many inputs for evapotranspiration calculation, each data point has the potential to adversely affect the final calculation.

Table 2. CIMIS Station# 245 reference data on four days

Day/Year/Time	08 Feb 2016 Noon/Cloudless	19 April 2016 Noon/Cloudless	22 June 2016 Noon/Cloudless	08 July 2016 Noon/Cloudless
Data Collected				
Total Precipitation (mm)	0	0	0	0
Average Solar Rad (W/m^2)	721.5	1018.6	1030.7	1025.9
Average Vapor Pres (kPa)	4.3	6.9	19.5	20
Average Air Temp (°F)	83.7	85	80.9	81.1
Average Relative Humidity (%)	11	17	54	55
Average Dew Point (°F)	35.5	35.5	60.8	61.2
Average Wind Speed (m/s)	5.0	3.6	4.1	3.8
Average Soil Temp (°F)	55.3	63.1	68.5	69.7
PM ET ($mm\ d^{-1}$)	0.16	0.25	0.25	0.25

4.2 Triangle Method Results

The Triangle method calculation was performed using the LDCM multispectral and thermal band calculations for 08 February, 19 April, 22 June, and 08 July 2016. The dates were specifically picked to fall on cloudless days as, close to noon as possible, measure NDVI when the evapotranspiration was at its highest potential as seen in Table 3. The actual evapotranspiration, as calculated by the Penman-Monteith method, was compared to the satellite evapotranspiration

method, as calculated by the Triangle method for the four days of measurement. Multispectral bands were used to calculate the greenness of a pixel relative to its neighbor. The NDVI was used to determine the satellite-based evapotranspiration for this project. NDVI values rise when more vegetation covers a pixel. This indicated by a rise in NIR reflectance and a fall in Red reflectance. The opposite is true when vegetation is sparse on non-existent. NDVI measures and shows the greenness of a pixel and is known to provide accurate evapotranspiration estimates (Rossato, et al. 2005).

NDVI values range from -1 to +1 with +1 indicating high vegetation cover and -1 indicating low vegetation cover. Thermal bands were manipulated to find the LST and converted from K to °C. The wet and dry edges of the triangle were annotated to reflect the placement of the pixel scatterplot. In the triangle method, the top of the opposite side indicates the least amount of evaporation, based on bare dirt. The point where the hypotenuse and adjacent side converge indicates where the greatest amount of transpiration occurs. To achieve this, LST and NDVI was calculated from the bands of the LDCM and placed on a two-dimensional plot as seen in Figure 12. To ensure the best reading possible, a Region of Interest (ROI) was specified to eliminate outliers. As a secondary check, classes were used to color code known areas of wet and dry such as golf courses, scrub land to reduce the error in selecting the triangle coordinates.

The accuracy and correlation between the Penman-Monteith method was greatly limited by the lack of measurable data for this project. For better accuracy, more data is required for a proper statistical analysis. Table 4 summarizes the variations between the measured Penman-Monteith values and the satellite-based evapotranspiration values. On the first day of measure, a large discrepancy occurred between the satellite and the measured evaporation. As the variables measured with the LDCM satellite did not capture weather conditions and were focused on the

measure of vegetation vigor, some variables that affect evapotranspiration on the ground may not be factored into the calculations. On the day in question (08 Feb 2016), there were wind gusts of up to 26 miles per hour. Wind plays a large part in the evaporation over a surface. In addition, the water restrictions for California, which limited heavy customer potable water use for watering, was still being enforced for the Coto De Caza Golf course. Because an orbiting body was used to measure evapotranspiration, which covered an entire region of interest and not two miles in radius as measured from the weather ground station, the numbers may have been inflated. Due to the ground station being a fixed point and the NDVI measure covers lakes, rivers, and other locations that may have irrigated, the readings, assumedly due to these factors, did not correlate. The results of the measurement are indicated in Table 4. This method has shown to closely track with actual evapotranspiration as measured by a weather station using the Penman-Monteith for evapotranspiration computation. This method should be considered as an acceptable method to develop a snapshot estimate of a measured area. However, when comparing it to a weather ground station, care must be taken if using only one. As each ground station is a study of the climate and conditions directly surrounding itself, while the NDVI Triangle method is more used for large-scale areas but not to that detail, caution must be taken if taken as actual readings against a single station.

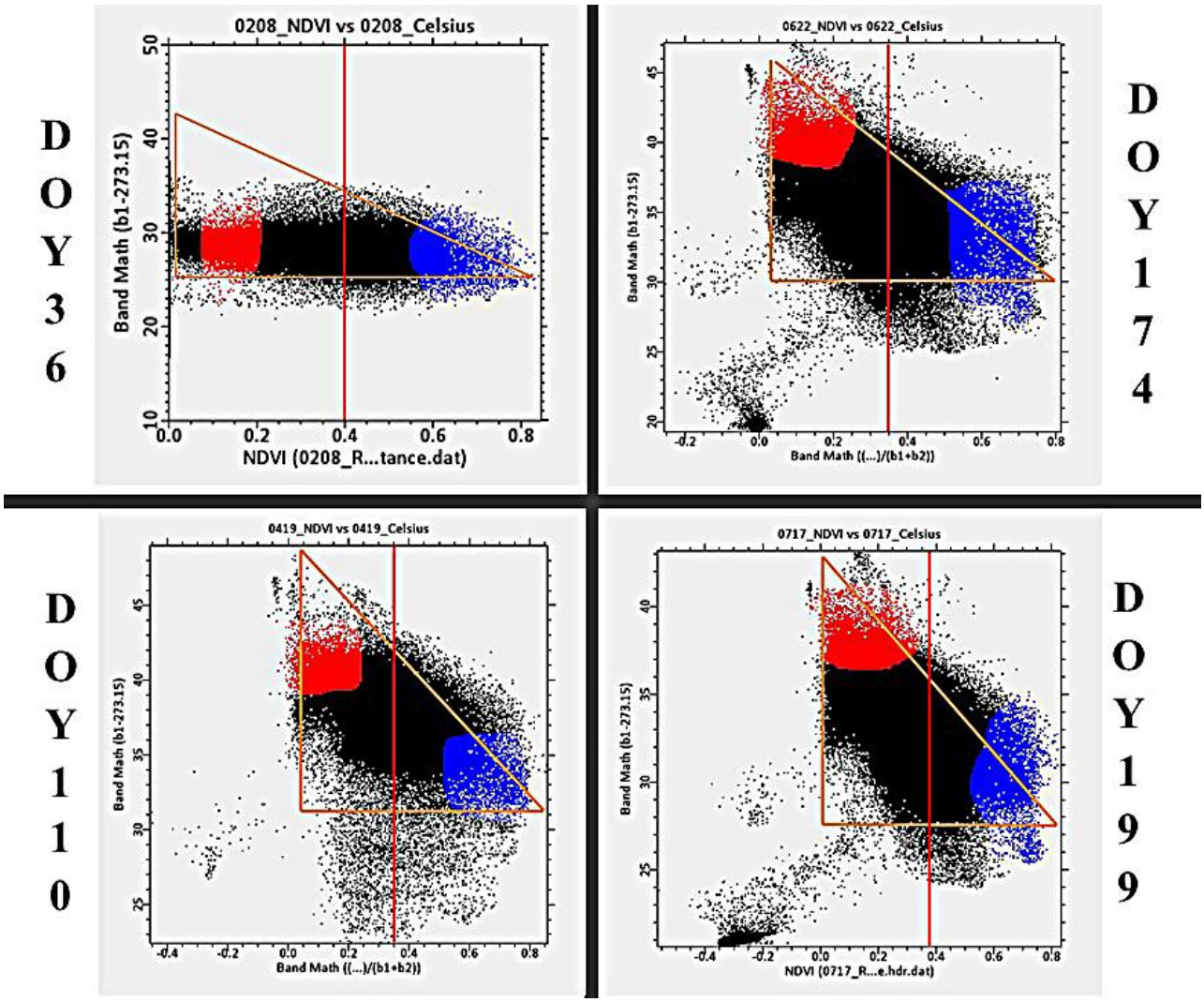

Figure 13 Two-dimensional scatter plots of satellite pixel values of NDVI versus the average of Top of Atmospheric (TOA) spectral radiance from LCDM satellite imagery (Source https://earthexplorer.usgs.gov/)

Table 3 Results of four days of NDVI Triangle Method calculations on a cloudless day

Day/Year/Time Cloudless	08 Feb 2016 10:22 a.m.	19 April 2016 11:28 a.m.	22 June 2016 11:28 a.m.	08 July 2016 11:28 a.m.
NDVI Index	0.4	0.35	0.35	0.37

4.3 Comparison of Methods

The Triangle method results were compared against the Penman-Monteith method to answer the question on whether the Triangle method could be used as a substitute for weather stations, which use the Penman-Monteith method, for evapotranspiration measurement. To find is the Triangle method was a suitable facsimile, the period, actual ET (Penman-Monteith), forecasted ET (Triangle Method), the error, the absolute value of error and square of error, and the absolute values of errors divided by the actual values. These values were then used to compute the Mean Absolute Deviation (MAD), the Root Mean Square Error (RMSE), $R^{\wedge 2}$, and the Mean Absolute Percentage Error (MAPE) as seen in Table 4.

Table 4 Penman-Monteith vs Triangle Method

Period/2016	Actual (Penman-Monteith)	Forecast (Triangle Method)	Error	Absolute Value of Error	Square of Error
1. 08 Feb	0.16	0.4	-0.24	0.24	0.0576
2. 19 Apr	0.25	0.35	-0.1	0.1	0.01
3. 22 Jun	0.25	0.35	-0.1	0.1	0.01
4. 08 Jul	0.25	0.37	-0.12	0.12	0.0144
	Totals	1.47	-0.56	0.56	0.092
	N = 4				

This project aimed to compare the two methods of calculating evapotranspiration statistically to determine the feasibility of using the NDVI Triangle method as an acceptable substitute for the Penman-Monteith model. However, with only four data points analyzed in this study, it is not feasible make any trusted statement on the NDVI Triangle Method.

Chapter 5 Conclusion

This study aimed to assess the effectiveness of estimating ET by comparing a ground-based method with a satellite-based method to determine the feasibility in using a satellite-based method for measuring ET. Using the generated study area, the satellite-based Triangle method can be used to estimate evapotranspiration for every area of the State of California that is not covered by a weather station. This research showed the geographic versatility of a satellite-based method of measuring ET when compared to a ground-based method. The main metric used to compare the data is a value called evapotranspiration which represents the water lost from the surface of the land (evaporation) and vegetation growth (transpiration). Together, these two values can be combined to estimate the total water loss from a land surface with vegetation cover. The remotely-sensed ET values were higher than those predicted by the Penman-Monteith method for the 4 days used in this study.

The NDVI Triangle method is an advanced-level method to generate evapotranspiration for a study area. The user must be intimately familiar with GeoTIFFs and the program of choice to extract the data into individual bands for evaluation. Band math knowledge and proficiency is critical for the calculation of SEBAL to obtain the values of NDVI and surface temperatures. The user must have knowledge of GIS as well as other mapping programs, and the ability to fully comprehend and execute the steps needed to integrate the multispectral and thermal bands for visualization. This method is not recommended for the medium to novice user and is impractical for the average GIS shop whose expertise is something other than satellite imagery analysis.

5.1 Discoveries

This study compared the Penman-Monteith method and the Triangle method suitability for estimating ET for the Moulton Niguel Water District. This project discovered satellite imagery is

the most versatile way to predict vegetation indexes as it has the capability of being very efficient when it comes to collecting and presenting data for diverse calculations of evapotranspiration. This provided confirmation that, when it is too difficult to obtain all the data sets needed to complete the Penman-Monteith measurements for evapotranspiration, remotely-sensed imagery can adequately fill the need. There has been many previous thoughts and methods on uses of remote satellite imagery to predict evapotranspiration. However, it still needs ground truth to confirm the data measured. In addition, satellite imagery is subjected to cloud cover and infrequent passes which make it great for an overall look and study of an area but poor due to the temporal delay from each pass. There have been only a few studies using remotely sensed data in a triangle form in a large-scaled area and compare it against the in-place weather station for the evapotranspiration value.

This study found the evapotranspiration values from the remotely-sensed station range from .35 to .4 inches of ET while the CIMIS weather station #245 measured evapotranspiration at a lower value range of .16 to .25 inches of ET. The trend matched on the months of April and June but diverged in February and July. It should be noted that in February, precipitation was at the lowest while in July, radiation was at its highest level. This may be due to the fact the ground-based weather station reading is greatly influenced by its direct surroundings while the satellite data, though measuring a large-scaled area, are not influenced by micro-climate weather and atmosphere changes. The Penman-Monteith method was directly created to measure evapotranspiration value shifts. Satellite data, using the Triangle Method, is subjective and requires the analyst to determine the wet and dry edges before it can be assumed where the value of evapotranspiration lie. The NDVI Triangle method, which is the measure of greenness in a pixel, with 30m resolution for the multispectral bands and 60m for the calculation of surface temperature, creates an estimation of evapotranspiration when the two are placed into a two-dimensional plot.

The two values, when placed on a plot, form a triangle consisting of a wet and dry edge for evapotranspiration measurement.

The difficulty of the SEBAL calculations for remotely-sensed imagery and the temporal latency of satellite passes, highlights the advantage local ground-based weather sensors have over orbiting bodies. The spatial inconsistencies are greater, 30m pixel to a point measurement for a ground-based weather station. However, the fact satellite data can measure large geographic tracts of land whose locations can be selected to regions of interest, show that advantage of the broadness of scope of evapotranspiration by orbiting bodies versus the more accurate but limited in area of measure ground unit.

5.2 Considerations and Limitations

One major limitation of this study is the fact that the wet and dry edge of the region of interest as measured using the NDVI Triangle Method is subjective and determined by the user. The surface land temperature must be calculated using the thermal bands of the satellite displayed against the NDVI, which is calculated through a series of steps. A second limitation was the number of days that were measured. Due to the study's focus on a region's clear cloudless day rather than a single pixel, accompanied by the LDCM's low rate of passes (every 16 days) This caused an inadequate amount of measured and matching cloudless days to the ground-based weather station, to definitively determine statistical error between the measured values. Other studies may opt to use a different orbiting body, one whose resolution is not as well as the LDCM but has more frequent passes. With additional data collected over a longer period and a more densely populated equation, a deeper assessment on how the Triangle method compares to the Penman-Monteith method of measuring evapotranspiration can be discovered.

Evapotranspiration is a very broad and complex concept, one that should be taken only if there is a single plan and track in place so that no distractions come in play. Originally this study did intend to utilize more than one station located within the Region of Interest (ROI) but, that station was inoperative at the time of measure. The additional station could have provided a more solid trend for the evapotranspiration values.

This study, with its limited data points, finds that there is no clear indication of agreement based upon the small number of readings taken. However, understanding the lack of data points, there is not a significant difference between the selected methods of measurement of evapotranspiration for the studied ROI. The NDVI Triangle method may provide comparable ET values when compared to ground-based weather stations. Locations that are remote, inaccessible or undeveloped may benefit from using free data to reasonably compute evapotranspiration by the NDVI Triangle method.

5.3 SWOT (Strengths Weaknesses, Opportunities, and Threats) Analysis

5.3.1 Strengths

The Penman- Monteith has many strengths as it is considered a world standard. It has been used globally to measure evapotranspiration in a variety climate condition for the last 50 years. With its multiple weather data sensor inputs from ground-based weather stations, it compensates for the smallest of change, ensuring even the slightest variation in weather is compensated and considered. It can measure and produce ET values on a minute-by-minute basis leaving no gap of information for the irrigator.

The NDVI Triangle Method strengths reflect its versatility in the size of land surface it can measure, and the myriad ways satellite imagery can be interpreted. This method, with its use of satellites, can provide current and historical ET values from any point of the globe. This data is free

to any user and can be accessed from anywhere in the world. The fact that no inventory, by the end user, is required for world-wide measurements makes this method extremely convenient and economical. When measuring ET, the NDVI Triangle method can produce an equivalent value without the need for a ground-based weather station assuming enough data has been collected.

5.3.2 Weaknesses

The Penman-Monteith method main weakness is the multiple sensor inputs for the equation. To gather that sensor data, a ground-based weather station, capable of taking all required weather readings must be available for use. These can be expensive and hard to maintain as each sensor needs to be calibrated regularly. Since these weather stations are so expensive, there are not enough to provide complete overlap of the areas measured for ET. In addition, this means locations, that cannot afford a weather station, will not be able to secure as accurate of a reading of a location that has a fully equipped weather. Weather stations can go dark as they are complicated instruments. This creates a gap in measurement or a discontinuation of data, altogether.

The NDVI Triangle uses satellites to measure ET. The fact there are so many selections can make the process more complicated as there are tradeoffs. Some satellites have very good resolution but a low pass rate while others have a daily pass, but the resolution is compromised in the process. Weather and cloud cover can prevent the satellite from creating a complete picture for ET values. While other ET measurements can be automated, the learning curve for SEBAL and the Triangle Method can be daunting.

5.3.3 Opportunities

The Penman-Monteith method relies on ground-based weather stations. Companies have taken the concept of a weather station and packaged it into a portable module which is disposable in tactical situations. These miniaturized versions of the large ground-based weather stations are

mobile, with interoperability with other like weather stations, via a cellular network, to increase the area being measured.

The NDVI Triangle Method can cover all areas of non-coverage without inventory cost, operating expense, or maintenance requirements. As climate change continues to cause variations in weather patterns, there will be a need for a wide-ranging method and inexpensive way to measure ET for all of California. This method may be the preferred option as local government's budgets are unaffected using satellite imagery.

5.3.4 Threats

The Penman-Monteith data for its equation comes from ground-based weather stations. These stations need to be set on irrigated land to provide accurate estimates of reference ET. If another drought occurs and water restrictions occur, there will be limited locations to place a weather station to measure ET. Many weather stations in California have been moved because the land they are situated upon is leased and when it expires, they must relocate. In addition, the Government's support of climate change is waning and that may affect the grants provided to fund these stations. Finally, methods using satellites may undermine the need for expensive and high maintenance weather stations.

Practitioners of the NDVI Triangle method may not have to directly pay for access to satellite imagery data but, there is an associated cost in keeping these in orbit. Satellites age, break in space where they cannot be fixed, lose orbit and are lost forever. Replacing a satellite or putting a constellation in orbit is prohibitively expensive and may only serve the sponsors of the satellite directly. Cloud cover and smoke from large fires remain a hindrance to accurately computing ET with satellite imagery.

5.4 Future Work

The study of using the NDVI Triangle to measure ET may be expanded to areas of California where CIMIS ground stations are more prevalent in the region. In the future, there should be an increased frequency of data collection from satellites to better resolve the accuracy of this method of measuring ET. If the temporal data points were increased and more densely populated, an accurate value would come from the additional comparative days. Future studies could also combine a set of weather stations in a region of interest and compare it to the region of interest. In that way, microclimate influence would be nullified by the integration of values from other stations outside that realm of weather influence.

A more pointed and directed study of a location, using a pixel as a point of study instead of and entire region, would include more LDCM's cloudless day passes required for this measurement. In turn, a more robust project conclusion and clearer refinement of the results could be established.

Studying evapotranspiration by continual comparisons of ground and satellite-based methods can give rise to a broad-based use of satellite imagery for evapotranspiration value measurements for remote areas that are either inaccessible or are unable to purchase expensive ground-based stations due to fiscal considerations.

REFERENCES

Allen, Kirk, Brown, Jennifer, Hachiya, Patricia, Skutecki, Lisa, Hernandez, Carolina, Chen, Tim. 2017. 2015 “Urban Water Management Plan for Los Angeles County Waterworks District 29, Malibu, and the Marina Del Rey Water System”. Department of Public Works. Waterworks Division. Alhambra, CA: County of Los Angeles.

Allen, Richard G., Albert J. Clemmens, Charles M. Burt, Ken Solomon, and Tim O’Halloran. 2005. "Prediction Accuracy for Project-wide Evapotranspiration Using Crop Coefficients and Reference Evapotranspiration". Journal of Irrigation and Drainage Engineering 131 (1): 24-36.

Allen, Richard G., Luis S. Pereira, Dirk Raes, and Martin Smith. 1998. "Crop Evapotranspiration – Guidelines for Computing Crop Water Requirements." FAO Irrigation and Drainage Paper 56. http://www.fao.org/docrep/X0490E/x0490e00.htm#Contents.

Anderson, Donald B. 1936. “Relative humidity or vapor pressure deficit”. Ecology 17:227 – 282.

Bastiaanssena, W.G.M., Menentia, A., Feddesb, R.A., Holtslagc, A.A.M. 1998. “A remote sensing surface energy balance algorithm for land (SEBAL). 1. Formulation”. Journal of Hydrology 212-213:198-212.

Beyazgül, M., Y. Kayam, and F. Engelsman. 2000. "Estimation Methods for Crop Water Requirements in the Gediz Basin of Western Turkey". Journal of Hydrology 229 (1-2): 19-26. doi:10.1016/s0022-1694(99)00196-1.

Blunden, Jessica. "Current Map." United States Drought Monitor. 2018. http://droughtmonitor.unl.edu/.

Cai, Jiabing, Yu Liu, Tingwu Lei, and Luis Santos Pereira. 2007. "Estimating Reference Evapotranspiration with The FAO Penman–Monteith Equation Using Daily Weather Forecast Messages". Agricultural and Forest Meteorology 145 (1-2): 22-35.

Crane, Fred, Conner P. Wallmark, Giang Hoang-Burdette, Carrie B. Reyes, Sarah Kolvas, Benjamin J. Smith, and Mary LaRochelle. 2018. "Golden State Population Trends." First Tuesday Journal. http://journal.firsttuesday.us/golden-state-population-trends/9007/.

Davis, S.L., and Dukes, M.D., 2012. "Landscape Irrigation with Evapotranspiration Controllers in a Humid Climate". Transactions of the ASABE 55 (2): 571-580.

Dickerson, Chris Ann, Ruth Thibodeau, Elliot Aronson, and Dayna Miller. 1992. "Using Cognitive Dissonance to Encourage Water Conservation". Journal of Applied Social Psychology 22 (11): 841-854.

Diffenbaugh, Noah S., Swain, Daniel L., Touma, Danielle. 2015. “Anthropogenic warming has increased drought risk in California”. Proceedings of the National Academy of Sciences of the United States of America. 112 (13) 3931-3936.

Ferguson, Bruce K. 1987. "Water Conservation Methods in Urban Landscape Irrigation: An Exploratory Overview". Journal of the American Water Resources Association 23 (1): 147-152.

GISGeography. 2018. “Spectral Signature Cheatsheet – Spectral Bands in Remote Sensing”. https://gisgeography.com/spectral-signature/.

Gleick, Peter H., Dana Haasz, Christine Henges-Jeck, Veenan Srinivasa, Gary Wolf, Katherine Kao Cushing, and Amardip Mann. 2003. "Waste Not, Want Not: The Potential for Urban Water Conservation in California." Pacific Institute.

Griffin, Daniel, and Kevin J. Anchukaitis. 2014. "How Unusual Is The 2012-2014 California Drought?” Geophysical Research Letters 41 (24): 9017-9023.

Han, Lijuan, Xiaowen Li, Jindi Wang, Shaomin Liu, and Ziti Jiao. 2004."A Simple Interpretation of NDVI-Ts Space Combining LAI and Evapotranspiration." IEEE International IEEE International IEEE International Geoscience and Remote Sensing Symposium. IGARSS 04. Proceedings. 2004 6 (2004): 3611-614. doi:10.1109/igarss.2004.1369899.

Liang, Shunlin, Li, Xiaowen, Wang, Jindi. 2012. “Advanced Remote Sensing.” Academic Press.

Johnson, Hans. 2017. "California's Population". Public Policy Institute of California. http://www.ppic.org/content/pubs/jtf/JTF_PopulationJTF.pdf.

Lillesand, Thomas, Ralph Kiefer, and Jonathan Chipman. 2012. “Remote Sensing and Image Interpretation”. 7th ed. Laser Words.

Lopez, Joone. 2017. "Moulton Niguel Water District Water Quality Report". MNWD 2016 Water Quality Report. https://www.mnwd.com/app/uploads/2017/06/2016-CCR_Water-Quality-Report_FINAL.pdf.

Loescher, H. W., C. V. Hanson, and T. W. Ocheltree. 2009. "The Psychrometric Constant Is Not Constant: A Novel Approach to Enhance the Accuracy and Precision of Latent Energy Fluxes through Automated Water Vapor Calibrations". Journal of Hydrometeorology 10 (5): 1271-1284.

Manivanan, R. 2006. “Recycling of Industrial Effluents”. New Delhi: New India Pub. Agency.

Marcus, Felicia, Steven Moore, Tam Doduc, Dorene D'Adamo, and E.Joaquin Esquivel. 2018. "Governor's Conservation Executive Orders and Proclamations." State Water Resources Control Board.

https://www.waterboards.ca.gov/water_issues/programs/conservation_portal/executive_orders.html.

McCarthy, Cara. 2017. “30-Year Climatic and Hydrologic Normals (1981-2010)”. U.S. Department of Agriculture, Natural Resources Conservation Service, National Geospatial Management Center. https://www.wcc.nrcs.usda.gov/normals/30year_normals_data.htm.

Monteith, John. 1965. "Evaporation and the Environment". Symposia of the Society for Experimental Biology. 19: 205 – 223.

Municipal Water District of Orange County (MWDOC). 2017. “Imported Water”. Your Water. https://www.mwdoc.com/your-water/.

Pidwirny, M. 2006. “Actual and Potential Evapotranspiration”. Fundamentals of Physical Geography. 2nd ed. Physicalgeography.net.

Rossato, Luciana, Alvala, Regina C.S., Ferreira, Nelson Jesus, Tomasella, Javier. 2005. “Evapotranspiration estimation in the Brazil using NDVIO data”. Proceedings of SPIE – The International Society for Optical Engineering 2005(5976):377-385.

Schmugge, Thomas, William Kustas, Jerry Ritchie, Thomas Jackson, and Al Rango. 2002. "Remote Sensing in Hydrology". Advances in Water Resources 25. http://ac.els-cdn.com.libproxy1.usc.edu/S0309170802000659/1-s2.0-S0309170802000659-main.pdf?_tid=8040c396-54a7-11e7-8391-00000aacb35e&acdnat=1497846584_f99e7bba6bf52352d9b2160188c61bbb.

Suleiman, Ayman A., and Gerrit Hoogenboom. 2007. "Comparison of Priestley-Taylor And FAO-56 Penman-Monteith for Daily Reference Evapotranspiration Estimation in Georgia". Journal of Irrigation and Drainage Engineering 133 (2): 175-182.

Suzuki, R and Masuda K., 2004. “Interannual Covariability Found in Evapotranspiration and Satellite-derived Vegetation Indices over Northern Asia”. Journal of the Metrological Society of Japan 82 (4), 1233 – 1241.

Tegos, A., Malamos, N., and Koutsoyiannis, D. 2015. "A Parsimonious Regional Parametric Evapotranspiration Model Based on A Simplification of the Penman–Monteith Formula". Journal of Hydrology 524: 708-717.

Temesgen, Bekele, Cayle Little, Jared Birdsall, Neil Rambo, and Ricardo Trezza. 2018. "CIMIS Overview." California Irrigation Management Information System. http://www.cimis.water.ca.gov/.

Temesgen, Bekele, Cayle Little, Jared Birdsall, Neil Rambo, and Ricardo Trezza. 2018. "Coto de Caza #245”. California Irrigation Management Information System. http://www.cimis.water.ca.gov/Stations.aspx.

TIGERweb. 2017."U.S. Census Bureau Quick Facts Selected. Orange County, California". Census.Gov. https://www.census.gov/quickfacts/fact/map/orangecountycalifornia/PST045216#viewtop.

Ward, F. A., and M. Pulido-Velazquez. 2008. "Water Conservation in Irrigation Can Increase Water Use". Proceedings of the National Academy of Sciences 105 (47): 18215-18220.

Westerhoff, R.S. 2015. "Using Uncertainty of Penman and Penman–Monteith Methods In Combined Satellite and Ground-Based Evapotranspiration Estimates". Remote Sensing of Environment 169: 102-112.

Willmott, Cort J., Scott M. Robeson, and Kenji Matsuura. 2011. "A Refined Index of Model Performance". International Journal of Climatology 32 (13): 2088-2094.

Woodford, Chris. 2017. "How Do Pyranometers Work | Thermopile and Solar-Cell Compared". Explain That Stuff. http://www.explainthatstuff.com/how-pyranometers-work.html.

Zotarelli, Lincoln, Michael Dukes, Consuelo Romero, Kati Migliaccio, and Kelly Morgan. 2009. "Step by Step Calculation of the Penman-Monteith Evapotranspiration (FAO-56 Method)". Agricultural and Biological Engineering Department, Florida Cooperative Extension Service, Institute of Food and Agricultural Sciences, University of Florida, no. AE459. http://edis.ifas.ufl.edu/pdffiles/ae/ae45900.pdf.

Appendix A Tables

Table 5. Summary of equipment and software needs for Normalized Difference Vegetation Index (NDVI) equation

Equipment/Software	Source	Application
ENVI	ENVI	Visualization/Analysis/ Data Organization
ArcMap	ESRI	Visualization/Analysis
ArcCatalog	ESRI	Data Organization
Sankey	www.Sankeymatic.com	Mode Flow Charts
S3	Amazon Web Services	Database Storage
Slack	Slack.com	Team Posting
USC Library Services	MyUSC	Research
Google Scholar	https://scholar.google.com	Research

Table 6 Download earth explorer Landsat Data Continuity Mission (LDCM) satellite imagery

Step One	Goto https://earthexplorer.usgs.gov/ for satellite data.
Step Two	Select location: MNWD – Centroid, Lat. 33.158269, Long. -117.268689
Step Three	Select date range
Step Four	Select data sets i.e. LDCM OLI/TIRS C1 Level-1
Step Five	Select additional criteria i.e. cloud cover
Step Six	Select results
Step Seven	Select area of interest for download
Step Eight	Download Level-1 GeoTIFF Data Product (967.1 MB)
Step Nine	Open “7 Zip”
Step Ten	Select *. Tar file
Step Eleven	Select “Open Inside”
Step Twelve	Extract data
Step Thirteen	Save to folder
Step Fourteen	Test data

Table 7 Calculation of Reflectance for study area using multispectral calculations

Step One	Open ENVI
Step Two	File open
Step Three	Select Shapefile
Step Four	Select file dropdown
Step Five	Open as Optical Sensor
Step Six	Select “LANDSAT”
Step Seven	Geotiff with Metadata
Step Eight	Open MTL File

Step Nine	Place shapefile over MTL in the Layer Manager
Step Ten	Goto tool box
Step Eleven	Select “Radiometric Calibration”
Step Twelve	Select “Multispectral “Calibration (ensure spectral subset indicates 7 out of 7 bands)
Step Thirteen	Select “file selection” in the right pane
Step Fourteen	Select the shape file
Step Fifteen	Click “OK”
Step Sixteen	Select “Reflectance in the Radiometric calibration”
Step Seventeen	Save as Reflectance
Step Eighteen	Remove MTL from the Layer Manager

Table 8 Calculation of Albedo from multispectral bands 1,2,3,4 and 5

Step One	Insert Band Math Expression = [((0.356*B1) + (0.130*B2) + (0.373*B3) + (0.085*B4) + (0.072*B5) -0.0018) / 1.016]
Step Two	Select Band 1 “Blue”
Step Three	Select Band 2 “Red”
Step Four	Select Band 3 “Infrared”
Step Five	Select Band 4 “Shortwave infrared 1”
Step Six	Select Band 5 “Shortwave infrared 2”

Table 9 Calculation of NDVI from Near Infrared (NIR) and Red multispectral bands

Step One	Insert Band Math Expression = [(b1-b2)/(b1+b2)]
Step Two	Select “Toolbox”
Step Three	Select “Reflectance” file
Step Four	Select Band 1 “NIR”
Step Five	Select Band 2 “Red”

Table 10 Resize data using pixel aggregation resampling methods

Step One	Select “Toolbox”
Step Two	Select “Resize Data”
Step Three	Select “Reflectance”
Step Four	Select “Spatial Subset” > (select map, 20 samples, 20 lines)
Step Five	Select “Red” & “Near Infrared”
Step Six	Select Layer Manager
Step Seven	Right click on resized data
Step Eight	Select “Quick Stats”
Step Nine	Copy the DN for band One, open Excel and paste band one data into new column. Repeat with band two
Step Ten	Highlight to select both columns and create chart/scatter plot
Step Eleven	Right click data line in chart
Step Twelve	Select “Add Trend Line”

Step Thirteen	Select “display equation on chart” and “display R-squared value on chart”
Step Fourteen	Copy the y intercept number on the chart
Step Fifteen	Click on the file name (The header information will appear on the right)
Step Sixteen	At the bottom click on "Spatial Subset" to subset all the bands in the image or "Spectral Subset" to choose one band to subset
Step Seventeen	"Spatial Subset" brings up another box for choosing the exact location of the subset
Step Eighteen	"Image" will bring up the image with a subset box that can be re-sized and moved around the image.

Table 11 Calculation of Weighted Difference Vegetation Index (WDVI) from multispectral bands 3, 4 and the y intercept from the resampled data

Step One	Insert Band Math Expression = B3-1.0157*B4
Step Two	Add equation B3-1.2337*B4 (the 1.2337 number comes from the Y intercept copied from the chart)
Step Three	Select Band 3 “Red” from calculated reflectance
Step Four	Select Band 4 “NIR” from calculated reflectance

Table 12 Calculation of the soil brightness correction L Value from NDVI and WDVI

Step One	Insert Band Math Expression = [(1-2*1.6-b11*b22)]
Step Two	Select Band 11 “NDVI”
Step Three	Select Band 22 “WDVI”

Table 13 Calculation of Soil-adjusted Vegetation Index (SAVI) from bands 3,4, and the L value

Step One	Insert Band Math Expression = ((B4-B3) *(1+B33))/(B4+B3+B33)
Step Two	Select Band 3 “Red”
Step Three	Select Band 4 “NIR”
Step Four	Select Band 33 “L” value

Table 14 Calculation of the Leaf Area Index (LAI) from the SAVI values

Step One	Insert Band Math Expression = [(11*(b44^3))]
Step Two	Select Band 44 “SAVI”

Table 15 Calculation of surface emissivity from calculated LAI

Step One	Insert Band Math Expression = [.986+0.004*b11]
Step Two	Select Band 11 “LAI”

Table 16 Calculation of Thermal Infrared (TIR) from LCDM multispectral bands 10 and 11

Step One	Select “Toolbox”
Step Two	Select “Radiometric Calibration”
Step Three	Select “Thermal Bands” (2 of 2 bands)
Step Four	Select “Spatial Subset”
Step Five	Select shapefile of study area
Step Six	In the radiometric Calibration box> keep “Radiance “selected

Table 17 Calculation of the canopy resistance to vapor transit (Rc) from both Thermal Infrared (TIR) bands

Step One	Insert Band Math Expression = [(((B1-0)/1) - ((1-b6) *1))]
Step Two	Select Band 1 “TIR” (check that the bands are 2/2)
Step Three	Select Band 6 “Emissivity”

Table 18 Calculation of Top of Atmospheric (TOA) spectral radiance from Band 10

Step One	Insert Band Math Expression = [((1201.14)/(alog(((b1*480.89)/b2) +1)))]
Step Two	Select Band 1 “Emissivity”
Step Three	Select Band 2 “Rc Band 10”

Table 19 Calculation of Top of Atmospheric (TOA) spectral radiance from Band 11

Step One	Insert Band Math Expression = [((1321.08)/(alog(((b1*774.89)/b2)+1)))]
Step Two	Select Band 1 “Enb”
Step Three	Select Band 6 “Rc Band 11”

Table 20 Conversion of TOA average temperatures from K to °C

Step One	Insert Band Math Expression = ((b10+b11)/2)
Step Two	Select Band 10 “LST B10”
Step Three	Select Band 11 “LST B11”

Table 21 Conversion to °C from K by adding absolute zero

Step One	Insert Band Math Expression = [B1-273.15]
Step Two	Select Band 1 “Average Temperature”